Screening for modulators of vesicular monoamine transporter 2 activity in cells using a fluorescent substrate

Master Thesis in Pharmacy

Inga Elise Tollan Sommer

Centre for Pharmacy and

Department of Biomedicine

University of Bergen

May 2022

Summary

Vesicular monoamine transporter 2 (VMAT2) is an essential protein for transport of monoamine neurotransmitters such as dopamine from the cytosol into synaptic vesicles, packing them for subsequent release into the synaptic cleft. Dysfunctional monoamine signalling disturbs neurotransmission and plays a role in several neurological diseases. Thus, VMAT2 holds therapeutic potential for the symptomatic treatment of these diseases. For example, in the case of chorea, a movement disorder associated with Huntington's disease, and tardive dyskinesia, inhibitors of VMAT2 that hinder the release of dopamine have already been approved. In Parkinson's disease where there is degeneration of dopaminergic neurons and loss of dopamine signalling, activators of VMAT2 have the potential to increase dopamine release and have been shown to be neuroprotective. We thus set out to establish a functional high-throughput screening assay that can help identify potential VMAT2 activators and inhibitors by using the fluorescent VMAT2 substrate FFN206, enabling the measurement of VMAT2 activity with a microplate reader. The screening assay uses HEK293 cells transiently transfected with human VMAT2 and is based on detection of increase or decrease of VMAT2-specific substrate uptake in the presence of different small molecule compounds. We screened the Prestwick chemical library® containing 1280 compounds, mainly FDA approved drugs, from which the initial screening gave 55 hits showing inhibitory or activating effects for VMAT2. All these initial hits were further evaluated with a concentration dependent substrate uptake assay to remove false positive hits from the initial screening and to investigate potency at lower compound concentrations. Top-ranking hit compounds were selected for further evaluation of EC_{50} and IC_{50} for VMAT2 and they were also assayed with human VMAT1, to determine their specificity for VMAT2. The screening and the consequent validation assays resulted in the identification of inhibitors of varying strength, in which prenylamine lactate is the most potent of them. The inhibitors also have a higher IC_{50} value for VMAT1 than VMAT2, indicating that they have a higher affinity for VMAT2. However, the activators did not show the same clear modulation of VMAT2. By using an inhibition displacement assay to check if the hit compounds compete with the known VMAT2 inhibitors dihydrotetrabenazine and salmeterol, we found that prenylamine lactate does compete with these known inhibitors, indicating that it binds to the same site in VMAT2.

Acknowledgements

This project was carried out at the Biorecognition research group (Department of Biomedicine, faculty of Medicine, University of Bergen), I would like to thank Prof. Aurora Martinez for giving me the opportunity to be a part of this group and work on my thesis here.

I would like to express my gratitude to my supervisors Dr. Svein Isungset Støve and Prof. Aurora Martinez for invaluable guidance throughout my thesis, without you none of this would have been possible. Thank you for all the support and everything you have thought me, and for always taking time to give guidance.

Knut Teigen, thank you for helping me with molecular clustering. I would also like to thank Ming, Dayne and all the other members of Lab E for creating a great work environment, and always providing your advice and sharing your expertise.

Thank you to my fellow master's students Gro and Marthe for the support and companionship.

I would also like to thank BioCat and Centre for Pharmacy at UiB for financially supporting my participation in the NBS contact meeting to present my work.

At last, I would like to thank my family and friends for the support and encouragement throughout my thesis.

Table of contents

List of abbreviations

BBB	Blood brain barrier
BOILED-Egg	Brain Or IntestinaL EstimateD permeation
CCPM1	Corrected count rate (counts per minute) for isotope 1
CNS	Central nervous system
COPD	Chronic obstructive pulmonary disease
D2-receptor	Dopamine 2 receptor
DA	Dopamine
DAT	Dopamine transporter
DHA1	Drug: H+ Antiporter-1 family
DMEM	Dulbecco's Modified Eagle's Medium
DSF	Differential Scanning Fluorimetry
dTBZ	Deutetrabenazine
DTT	DL-Dithiothreitol
EC_{50}	The half-maximal effective concentration
FBS	Fetal bovine serum
FDA	U.S Food and Drug Administration
FFN206	Fluorescent false neurotransmitter 206
HD	Huntington's disease
HEK	Human embryonic kidney
HTBZ	Dihydrotetrabenazine
HTS	High-throughput screening
hVMAT2	Human vesicular monoamine transporter 2
hVMAT2-GFP	Human vesicular monoamine transporter 2 - green fluorescent protein
IBS	Irritable bowel syndrome
IC_{50}	The half-maximal inhibitory concentration
LB	Luria-Bertani broth
MAO-B	Monoamine oxidase B
MFS	Major facilitator superfamily
NET	Noradrenaline transporter
ORF	Open reading frame
PAINS	Pan-assay interference compounds
PBS	Phosphate buffered saline
PBS-T	PBS with tween-20
PCR	Polymerase chain reaction
PD	Parkinson's disease
PNS	Peripheral nervous system
RAAS	Renin angiotensin aldosterone system
SB	Laemmli sample buffer
SDS-PAGE	Sodium dodecyl sulphate polyacrylamide gel electrophoresis

SERT	Serotonin transporter
SLC18	Solute carrier
SOC	Super optimal broth with Catabolic repression
STD	Standard deviations
TBZ	Tetrabenazine
TD	Tardive dyskinesia
TM	Transmembrane
VAChT	Vesicular acetylcholine transporter
VBZ	Valbenazine
VMAT	Vesicular monoamine transporter
VPAT	Vesicular polyamine transporter
[^{3}H]-HTBZ	[^{3}H] dihydrotetrabenazine
α-HTBZ	Alfa-dihydrotetrabenazine
β-HTBZ	Beta-dihydrotetrabenazine
5-HT	Serotonin

1 Introduction

1.1 Vesicular monoamine transporter

Synaptic transmission requires the release of neurotransmitters from the presynaptic neuron into the synaptic cleft, allowing them to bind to receptors on the postsynaptic neuron that subsequently results in signal transduction (1, 2) (Figure 1.1). For neurotransmitters to be released into the synapse, the membrane potential of the neuron must be depolarized by an action potential, opening the voltage-gated Ca^{2+}-channels and generating an influx of Ca^{2+} that activates exocytosis of the neurotransmitters into the synaptic cleft from the synaptic vesicles they are stored in (3). Termination of neurotransmitter signalling occurs by enzymatic inactivation at the synapse, by reuptake of the neurotransmitters into the presynaptic terminal or neighbouring glia cells by sodium and chloride coupled membrane transporters, or by simple diffusion of the neurotransmitter away from the synapse. Neurotransmitters that are taken up from the synaptic cleft are recycled and packed into synaptic vesicles together with newly synthesised neurotransmitters by vesicular monoamine transporter 2 (VMAT2) for subsequent neurotransmission (4).

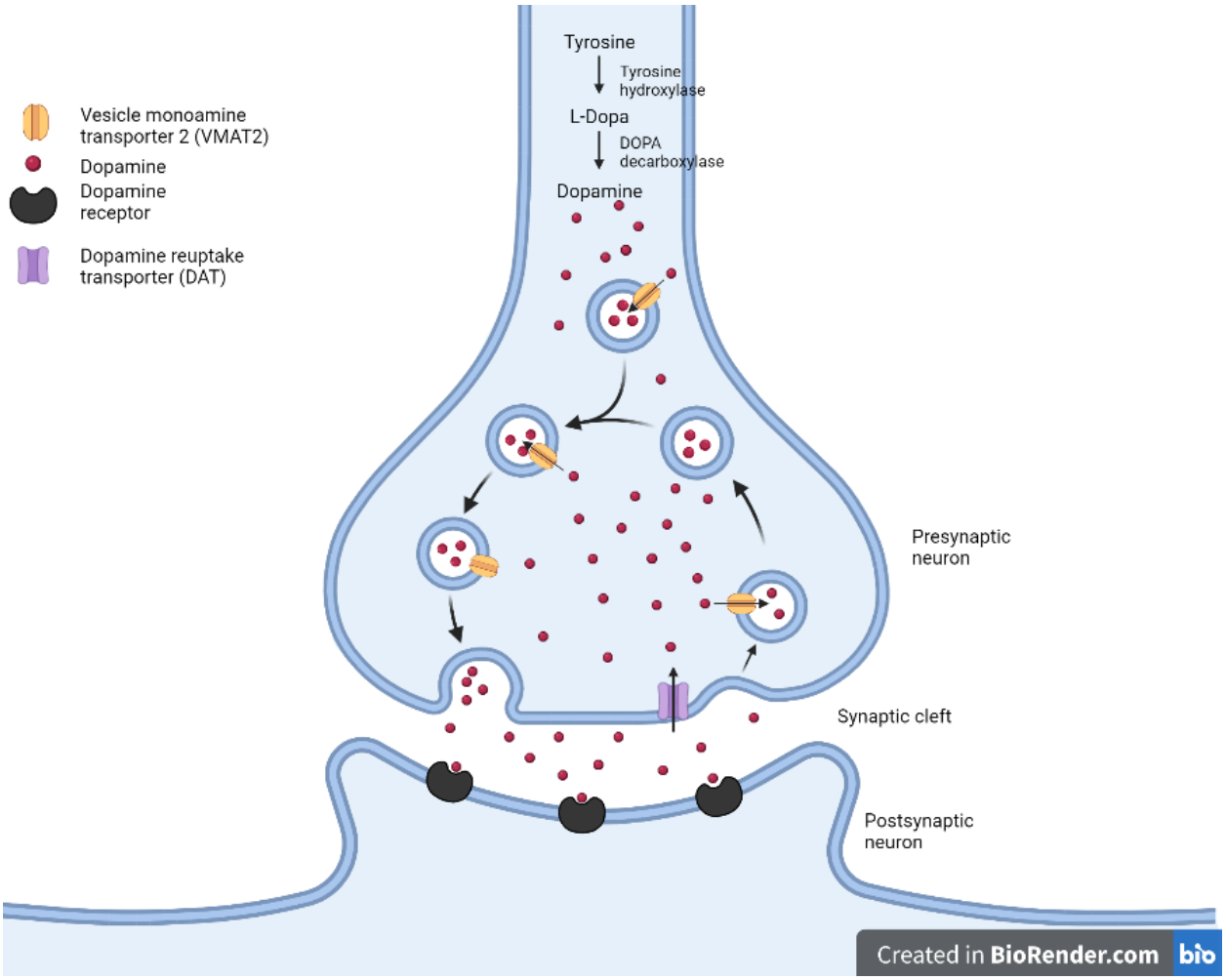

Figure 1.1 ***Schematic representation of the dopamine signalling pathway.*** *Dopamine is synthesised from tyrosine in the presynaptic neuron, before being transported into synaptic vesicles by VMAT2. The synaptic vesicle merges with the membrane, releasing dopamine into the synaptic cleft for subsequent neurotransmission. The dopamine signalling is either ended by reuptake into the presynaptic neuron for reuse, represented in the figure, or by other pathways not represented. Created with BioRender.com.*

The vesicular monoamine transporter (VMAT) is responsible for the active transport of the monoamine neurotransmitters, dopamine (DA), serotonin, adrenaline, noradrenaline, and histamine from the cytosol and into the vesicles (1). The active transport of the monoamines against the concentration gradient performed by VMAT is H^+-coupled as it relies on the proton electrochemical gradient generated by the vesicular H^+-ATPase (1), where two protons move in the opposite direction of each monoamine neurotransmitter that is packed into the synaptic vesicles (5) (Figure 1.2). The H^+-electrochemical gradient generation is coupled to hydrolysis of ATP by the H^+-ATPase (2), which is also referred to as V-ATPase (6).

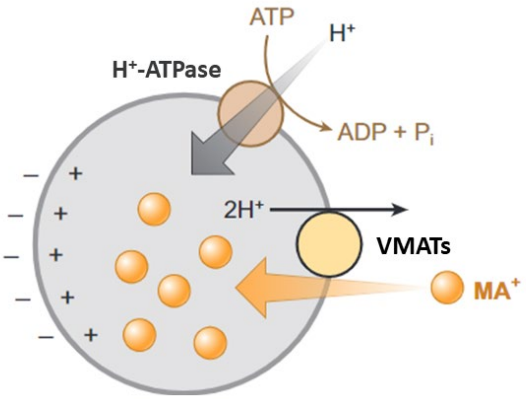

Figure 1.2: ***Transport of monoamines into a synaptic vesicle.*** *Each monoamine neurotransmitter (MA^+) transported into the synaptic vesicle is exchanged for two protons. This transport against the electrochemical concentration gradient is dependent on the hydrolysis of ATP to ADP by the H^+ ATPase, which generates a proton gradient. Figure modified from (2).*

1.1.1 VMAT1 and VMAT2

VMAT has two isoforms, VMAT1 (SLC18A1) and VMAT2 (SLC18A2) (5). VMAT1 is mainly expressed in neuroendocrine cells in the peripheral nervous system (PNS) (3), but also in rodent brain (7). In contrast, VMAT2 is mainly expressed in the central nervous system (CNS), in neurons, but also in PNS, in mast cells, pancreatic β-cells, adrenal chromaffin cells, blood platelets and enteric cells containing histamine (3). Both isoforms transport monoamines into storage vesicles, but most monoamines have higher affinity towards VMAT2 than VMAT1 (2), and histamine can only be transported by the VMAT2 isoform (1). Human VMAT1 and VMAT2 have high sequence homology (63.55% sequence identity determined with Clustal2.1) (8) with higher sequence identity in the transmembrane regions, and larger differences in the cytoplasmic N- and C-terminals and the ~87 aa long vesicular loop (residues 42-129 in VMAT2) (UniProt Q05940) (Appendix Figure 9.1). In Figure 1.3 the AlphaFold models of VMAT1 (cyan) and VMAT2 (light orange) are superimposed (9, 10). When comparing the transmembrane (TM) α-helixes, one can see that the structures of VMAT1 and VMAT2 are similar. The biggest differences between the structures are in the N- and C-terminals, and in the large vesicular loop which has low confidence of the predictions according to AlphaFold (9, 10), so it is difficult to confidently assess how different the two isoforms are in those regions.

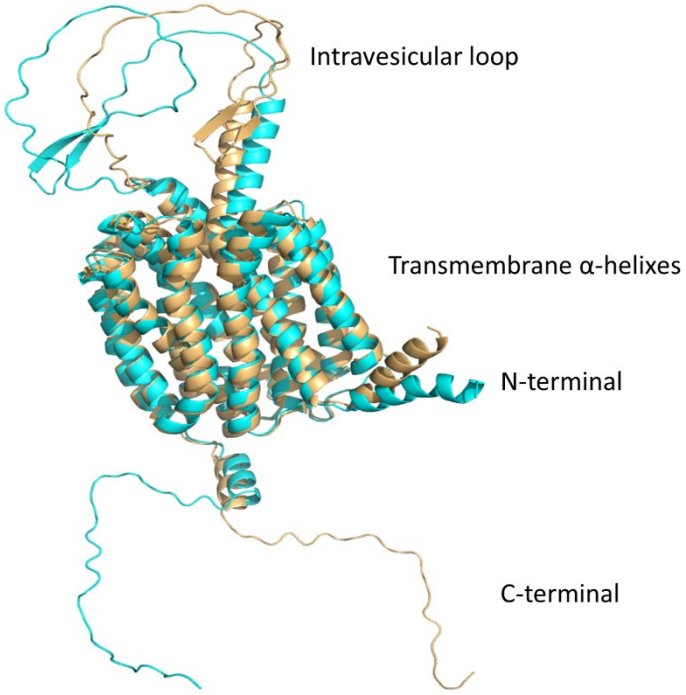

Figure 1.3: ***Comparison of the predicted structures of human VMAT1 and VMAT2 by AlphaFold.*** *VMAT1 (cyan), and VMAT2 (light orange). The N- and C-terminals, and the large intravesicular loop have low confidence in the AlphaFold prediction, and it is therefore difficult to conclude how different the two isoforms are in those regions. For the transmembrane α-helixes of the structures there are not any major differences between the transporters. Structures from AlphaFold (9, 10).(https://alphafold.ebi.ac.uk/entry/Q05940 and https://alphafold.ebi.ac.uk/entry/P54219)*

1.1.2 Structure of VMAT

The VMATs are members of the major facilitator superfamily (MFS), the largest family of secondary active transporters, which includes antiporters, symporters, and uniporters (1). The solute carrier family (SLC) consists of 65 families (6), where approximately one third belong to MFS (11). VMATs are members of SLC18, other members are the vesicular acetylcholine transporter (VAChT) (1, 12), and vesicular polyamine transporter (VPAT) (13). The SLC18 family is a subclass of Drug: H^+ Antiporter-1 family (DHA1), where the transport performed by the antiporters in this family requires exchange of two protons (12). The highly studied SLC6 family of monoamine transporters responsible for reuptake of VMAT2 substrates from the synapse on the other hand, are dependent on the sodium gradient. Members of the SLC6 family such as the dopamine transporter (DAT), noradrenaline transporter (NET) and serotonin transporter (SERT)

are localised in the membrane of presynaptic neurons, carrying out reuptake of dopamine, noradrenaline and serotonin from the synaptic cleft (6) (Figure 1.1).

Contrary to what is known about DAT and SERT (14-17), the structure of VMAT has not yet been determined experimentally, but there are available homology models based on structures of bacterial MFS transporters (18, 19) and models predicted by AlphaFold (9, 10) (Figure 1.3). VMAT is an antiporter that consists of 12 TM α-helixes divided in to two bundles with a large intravesicular N-glycosylated loop between the two first TM α-helixes (20) (Figure 1.4B and C). The N-terminal domain consists of the TM-α helixes 1-6 and the C-terminal domain of TM-α-helixes 7-12 (1), with both the C- and N-terminal located in the cytosol (20) (Figure 1.4A). There is a pseudo-two-fold symmetry between the two domains of the transporter, with the axis running normal to the membrane between the C- and N-terminal domain. There is also a similarity for the TMs where the six TMs in N-term six TM bundle (Figure 1.4A) has a twofold symmetry, the same applies to the TMs in the C-term six TM bundle (Figure 1.4A),with the axis running parallel to the membrane through the centre of the domains (1, 20).

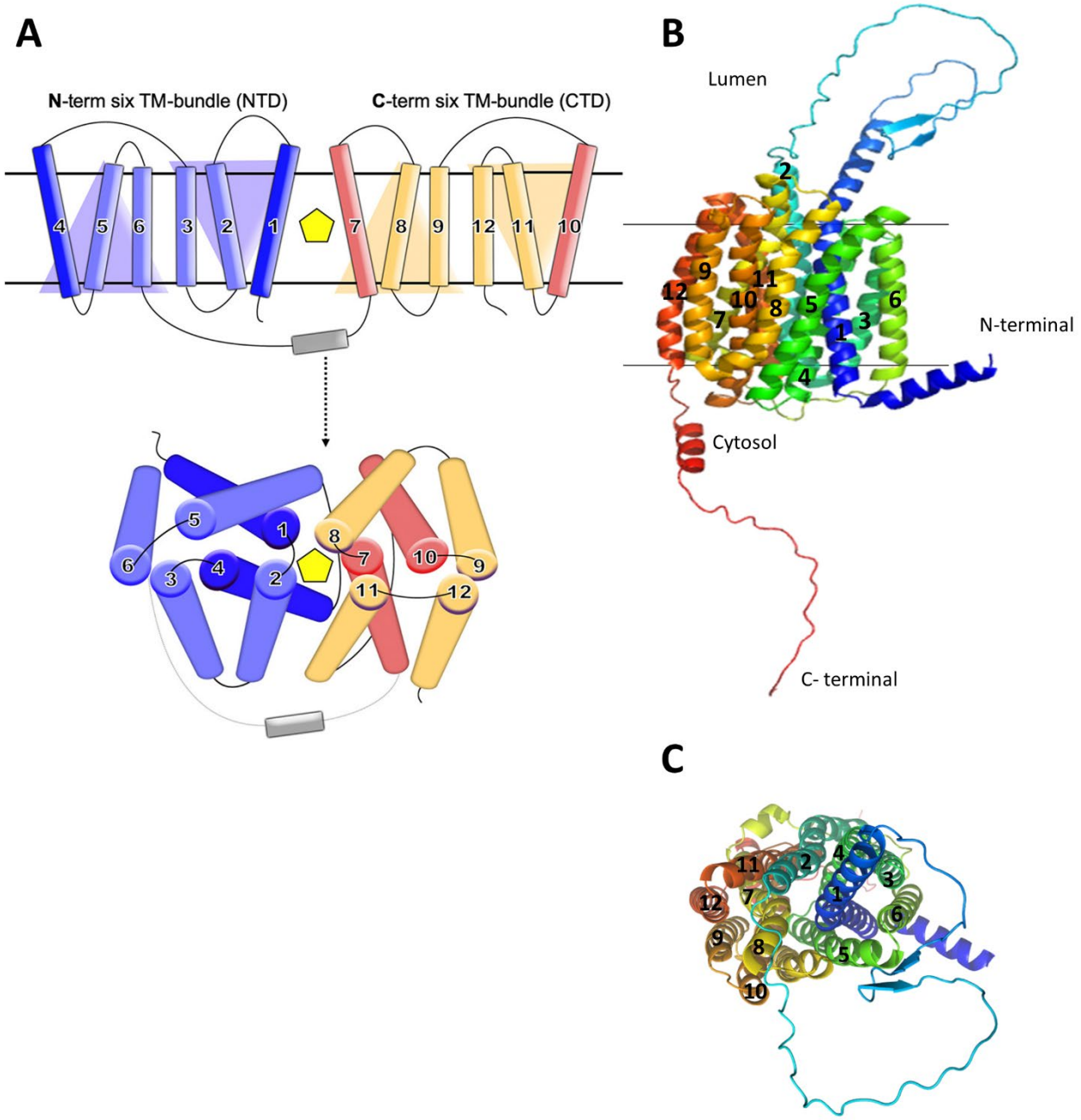

Figure 1.4: ***Overview over the structure and symmetry of VMAT*** *A: Illustration of the 12 transmembrane helixes of VMAT, where the TMs in N-term six TM bundle are structurally related; the same applies to the TMs in C-term six TM-bundle. There is also a pseudo two-fold symmetry between the N-terminal domain and the C-terminal domain. B: Model of human VMAT2, showing the glycosylated loop and the C- and N-terminals. C: Model of VMAT2 from B, seen from above, illustrating the symmetry in A. A: Figure from (21) , B and C: Structural model from AlphaFold (9, 10).*

For every cycle of monoamine transport, VMATs undergo several conformational changes. The mechanism behind these changes is the alternating access mechanism (Figure 1.5), allowing only one side of the transporter to be available for substrates at the same time. The conformational change is dependent on binding of a proton or substrate to the transporter. Binding of a proton

changes the "opening" from the lumen facing side, to the cytoplasm facing side with a rocker switch manoeuvre, whereas binding of a substrate induces a conformational change back to the lumen conformational stage where the substrate is released (1).

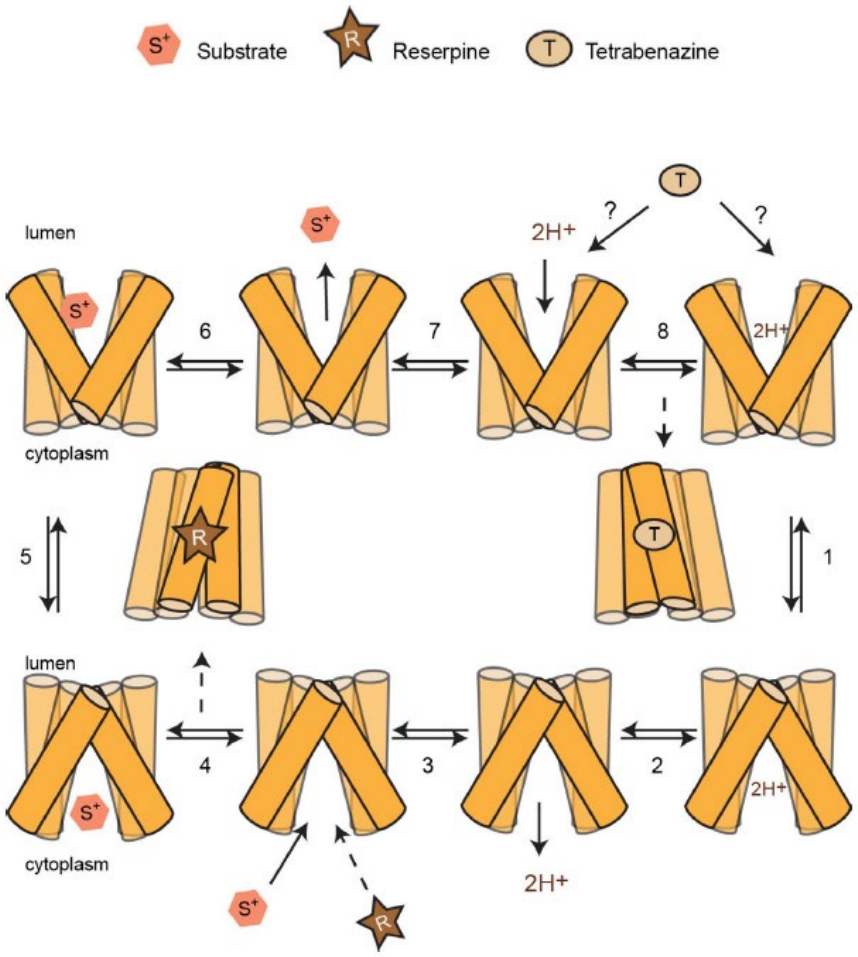

Figure 1.5: ***Illustration of the alternative access mechanism, and the different steps during the functional conformational change.*** *The figure is simplified by only showing six TMs, instead of twelve. Binding of protons in the lumen facing state (top of the figure) to the transporter changes the conformation to the cytoplasm facing state (bottom of the figure), releasing the protons and allowing for substrates (S^+) to bind. The binding of substrate returns VMAT to the lumen facing state, releasing the substrate into the vesicle. The binding site of the inhibitor tetrabenazine (T) is in the lumen facing state, ending in a dead-end complex, illustrated next to step 1. The inhibitor reserpine (R) competes with substrates for the binding site in the cytoplasm facing state, illustrated with the dashed arrow. Binding of reserpine also ends in a dead-end complex, shown next to step 5. Figure from (1).*

Reserpine and tetrabenazine (TBZ), two known VMAT2 inhibitors which are discussed in more detail below, display two slightly different binding sites of VMAT2 (Figure 1.5). The inhibition mechanism by TBZ involves two steps ending in a dead-end complex, where TBZ probably binds to VMAT2 in the lumen facing state (1). Reserpine binding also ends in a dead-end conformation, but it seemingly binds to the cytoplasm facing side as it competes with substrates (Figure 1.5). To

display the high affinity binding site of reserpine, it is proposed that translocation of a proton is necessary, as reserpine binding is accelerated by the presence of a proton gradient (1).

1.2 The monoamine neurotransmitters transported by VMAT

Monoamine neurotransmitters accumulate in synaptic vesicles by VMAT2, for subsequent neurotransmission (1). All monoamines are synthesized from the aromatic amino acids phenylalanine and tyrosine (DA, noradrenaline and adrenaline), tryptophan (serotonin) and histidine (histamine) (22-24) (Figure 1.6)

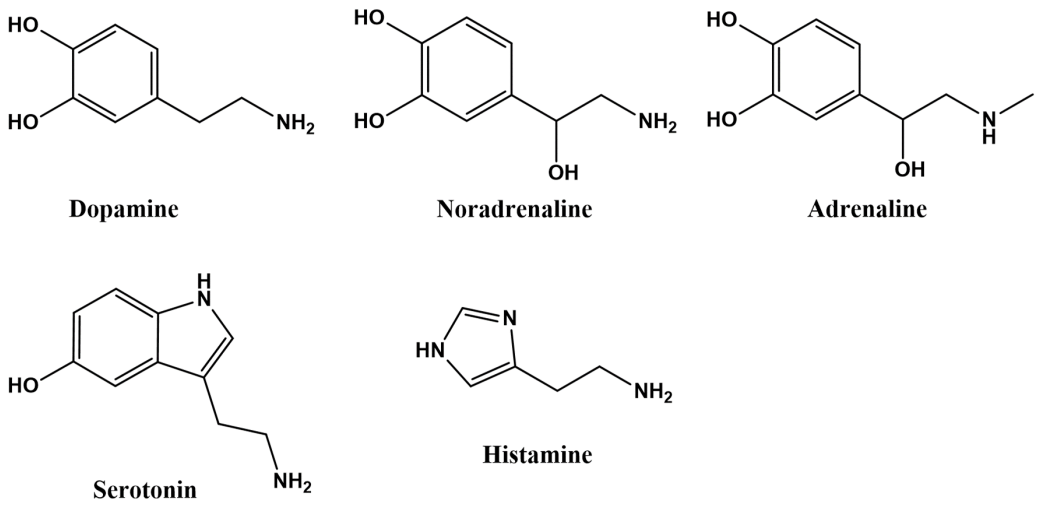

Figure 1.6: ***The monoamine neurotransmitters transported by VMAT.*** *Histamine is only transported by VMAT2, while the other neurotransmitters are transported by both VMAT1 and VMAT2.*

1.2.1 Dopamine

DA is a neurotransmitter involved in several physiological functions such as mood, cognition, and movement, and is synthesised in the cytosol in both the CNS and the periphery. Tyrosine is the precursor of DA and is absorbed from protein-rich food, or synthesised from L-phenylalanine by phenylalanine hydroxylase. Tyrosine is then converted into L-DOPA by tyrosine hydroxylase, which in turn, is further converted to DA by the enzyme aromatic L-amino acid decarboxylase (25).

Due to the crucial functions of DA, dysfunction of the dopaminergic system plays a role in several diseases, including Parkinson's disease (PD) (26), and depression, as further discussed later. DA also has important roles in neuroendocrine cells and neuronal fibres in the periphery, where it can regulate insulin secretion, food intake and even respiration(27).

1.2.2 Noradrenaline and adrenaline

Noradrenaline is synthesised from DA inside the synaptic vesicles by dopamine β-hydroxylase (23, 28) and thus, the inhibition of DA transport by VMAT2 can also lead to the reduction of noradrenaline. The noradrenergic system is known for the "fight or flight" response and in the CNS, it promotes wakefulness and arousal, but it has also been shown to affect some aspects of cognition and behaviour (23). In the presynaptic terminal of neurons containing phenylethanolamine-N-methyl transferase, noradrenaline is either released or converted to adrenaline (23). Adrenaline is also involved in the "fight or flight" response together with noradrenaline and so stress activates the synthesis and secretion of these catecholamines (29).

1.2.3 Serotonin

Serotonin (5-HT) is a neurotransmitter modulating a variety of neuropsychological process such as anger, attention, aggression, appetite, reward and memory, and is important in nearly all brain functions, but it is also common outside the CNS (30). Over-activity caused by excess serotonin at synapses in the CNS and PNS is toxic and can cause serotonin syndrome, which is potentially fatal. Symptoms range from mild to severe, and include agitation, hypothermia and rigidity (31). Increased cytosolic serotonin in the neuron can also result in the formation of reversible spheroids at serotonergic neurites (32). Daubert et al. demonstrated that these spheroids form with increased synthesis of serotonin and inhibition of VMAT2 by reserpine. These spheroids can form likely due to autophagic limitations and ubiquitination because of increased cytosolic 5-HT (32).

1.2.4 Histamine

Histamine has a key role peripherally in allergic reactions but is also important in CNS. The histaminergic system in the CNS is involved in several functions, such as cognitive functions and suppression of eating (33). Histamine is only transported by VMAT2, and not VMAT1(1), but the exact role of VMAT2 in the histaminergic system is not well studied (34).

1.3 Vesicular monoamine transporter 2 in disease

The accumulation of monoamine neurotransmitters into synaptic vesicles by VMAT2 is an essential step in neurotransmission. In fact, dysfunctions in monoamine neurotransmission are linked to several psychiatric and neurological diseases such as PD, Huntington's disease (HD) and depression (5). Thus, due to the critical role of VMAT2 in neurotransmission, it is a potential therapeutical target to treat these neurological diseases.

1.3.1 Activation of VMAT2 as a potential treatment of Parkinson's disease

1.3.1.1 Parkinson's disease

PD is a progressive neurodegenerative disease, with progression varying from slow to rapid forms (35), characterized by movements issues, such as rigidity, tremor, and slowness. The major pathophysiological characteristic of PD is the presence of Lewy bodies, which are neuronal inclusion bodies consisting mainly of α-synuclein protein aggregates that are associated with death of the DA producing dopaminergic neurons in the *substantia nigra,* the main source of DA in CNS (35, 36). Although the dopaminergic neurons are most severely affected, neurons that produce other neurotransmitters such as acetylcholine, serotonin, and noradrenaline neurons can also be affected (35).

PD is considered as a multifactorial disease, and the causative mechanism behind DA neurodegeneration and PD development is currently not known. DA dysregulation can be one contributing factor as increased cytoplasmic levels of DA lead to higher DA metabolism, which in

turn results in the generation of toxic reactive oxygen species (ROS) (37-39) as cytosolic dopamine is degraded by autoxidation or by enzymatic deamination to harmful reactive oxidative metabolites (5). Dopaminergic neurons have high iron and low antioxidant level, and is therefore thought to be exposed to oxidative stress (36). Because cytosolic DA is toxic, the packaging of DA into synaptic vesicles is critical and thus increased VMAT2 activity is shown to be neuroprotective (5).

The only available treatments of PD are symptomatic treatments that have no effect in preventing disease progression or maintaining normal neurotransmission and neuronal integrity (5). The main treatment of PD is supplementation of the DA precursor levodopa (therapeutic, synthetic L-DOPA), that can cross the blood-brain barrier and is converted to DA by the enzyme aromatic L-amino acid decarboxylase, causing a burst of DA signalling in DA neurons (40). Levodopa replaces the loss of DA temporarily but has a reduced effect over time, as a consequence of changes in the brain. The ability to store extra DA decreases, and both the long-term and short-term response to dopaminergic medicines also decreases (5, 35).

Having enough cytosolic DA is, however, not sufficient if DA cannot be transported into synaptic vesicles by VMAT2 for further neurotransmission. Thus, VMAT2 modulators that increase transporter function have potential to be combined with levodopa treatment for symptomatic treatment of PD (5). However, levodopa treatment comes with a risk for dyskinesia, called levodopa-induced dyskinesia (35) and thus other medications are now also used for treatment of PD, including DA agonists, that bind directly to dopamine 2 (D2) receptors (41), monoamine oxidase-B (MAO-B) inhibitors that increase DA signalling by reducing DA breakdown in the cytoplasm (35), and anticholinergic agents that are competitive antagonists for the muscarinic receptors (42). Treatment with DA agonists and MAO-B inhibitors are associated with a lower risk of dyskinesia, but several patients using DA agonist experience impulse control disorders, such as gambling, and those who use MAO-B inhibitors experience less symptom relief compared to levodopa treatment. Anticholinergics are used with caution due to adverse effects related to cognition (35).

The DA receptor agonist pramipexole used in treatment of PD prevents loss of dopaminergic neurons and increases the packaging of DA into synaptic vesicles (2) but it does not stop disease

development. In the study performed by Antonini et al., 72% of the patients in the pramipexole treatment group needed additional treatment with levodopa after four years. Like with other DA agonists, the use of pramipexole also comes with adverse effects such as nausea (43). However, pramipexole is able to drastically reduce parkinsonism in patients with the VMAT2 mutation Pro387Leu that leads to decreased activity of the protein and thus the loss of monoamine accumulation into synaptic vesicles (44).

1.3.2 Inhibitors of VMAT2 have a therapeutic effect in patients with tardive dyskinesia and chorea associated with Huntington's disease

An imbalance in DA signalling in the motor striatum is the cause of tardive dyskinesia (TD) (45). The physiology behind TD is not entirely known, but the prevalent theory is that DA antagonists cause an increased sensitivity for DA for the D2 receptor in the indirect pathway of motor striatum (45-47). Most likely the long-term blockade of the D2 receptor by this medication results in reduced degradation of D2 receptors and/or increased synthesis and density of D2 receptors which again will result in increased DA sensitivity (46).

Inhibition of VMAT2 reduces the packing of DA from cytoplasm and into the synaptic vesicles, which further leads to a reduced amount of DA being released into the synaptic cleft (48). Inhibition of VMAT2 also leads to increased degradation of DA in the presynaptic nerve terminal, which prevents the build-up of DA (46). This decrease is what is thought to be the reason for the reduction of TD, due to the reduction in DA signalling in nigrostriatal pathway (48).

Inhibitors of VMAT2 are used today to treat tardive dyskinesia (TD) which is a side effect of antipsychotics, and chorea associated with Huntington's disease (3, 47, 48). There are three VMAT2 inhibitors approved by the US Food and Drug administration (FDA) – TBZ, valbenazine (VBZ) and deutetrabenazine (dTBZ) (3)**.** TBZ is used to treat chorea associated with HD and VBZ is approved for use to treat TD, while dTBZ is approved for both TD and chorea associated with HD (3).

1.3.3 Known modulators of VMAT2 activity

1.3.3.1 Reserpine

Reserpine, along with TBZ, which will be described in more detail in Section 1.3.3.2, is the most studied VMAT inhibitor (3). Reserpine was initially identified in 1952, and is an alkaloid extracted from the snakeroot *Rauwolfia serpentine*. It was initially used as an antihypertensive and antipsychotic therapeutic and is a competitive inhibitor binding with very high affinity and quasi-irreversibly to both VMAT1 and VMAT2 (5, 49). Due to adverse side effects observed with the clinical use of reserpine, its use today is limited (3, 5), and is now mainly used in veterinary medicine (1). The most common side effects linked to reserpine use are parkinsonism and depression due to its ability to inhibit VMAT1 and VMAT2, subsequently resulting in the depletion of the neurotransmitters serotonin, noradrenaline and DA (3, 5). Apart from this, the irreversible binding of reserpine to VMAT poses another challenge for its clinical use, as new VMAT proteins need to be synthesised to reverse the effect, and thus it could potentially take several weeks to wash out the drug from the patient's system (5).

1.3.3.2 Tetrabenazine and tetrabenazine isomers

Tetrabenazine (TBZ) is another well-studied VMAT inhibitor (3), but unlike reserpine which binds quasi-irreversibly and competitively to both VMAT1 and VMAT2 (5, 49), TBZ binds reversibly and non-competitively to only VMAT2 (3). The selective binding of TBZ to VMAT2, and not VMAT1 is the likely reason as to why it is not associated with peripheral side-effects in the same manner as reserpine. Using therapeutic doses of TBZ, it is mainly DA that cannot accumulate into synaptic vesicles (45). As mentioned earlier, VMAT2 has two conformations: a cytoplasm- and a lumen- facing conformation (Figure 1.5). Unlike reserpine which binds to the cytoplasm facing conformation of VMAT2, TBZ binds to the lumen facing one, resulting in the formation of a dead-end complex where the transporter is unable to convert to the cytoplasm facing conformation, thus effectively inhibiting the transport of neurotransmitters into the vesicle (3).

In vivo, TBZ is converted into two metabolites with both positive and negative isomers of each and with different half-lives ranging from two to eight hours, which requires TBZ to be administrated

three times daily (47). The two metabolites are alpha-dihydrotetrabenazine (α-HTBZ) and beta-dihydrotetrabenazine (β-HTBZ), where the positive metabolites (+)α-HTBZ and (+)β-HTBZ have the highest affinity towards VMAT2, while the negative isomers (-)α-HTBZ and (-)β-HTBZ affect the D2-receptor and 5-HT receptors in addition to VMAT2 (3).

Apart from the short half-life of TBZ, another challenge with the therapeutic use of this compound has been the reported adverse effects experienced by patients, such as parkinsonism, depression and somnolence (50). It has been hypothesised that depression is caused by a reduction of DA, serotonin and noradrenaline levels (51) and thus it is possible that the use of TBZ does not only lead to a reduction of exocytotic DA release, but also serotonin and noradrenaline. In fact, TBZ comes with a box warning for suicidality and depression for HD patients (3).

The need for frequent dosing as well as the reported side effects associated to TBZ use have led to the development of deutetrabenazine (dTBZ), in an attempt to overcome these challenges (50). dTBZ is a compound structurally-related to TBZ that contains deuterium and has the same metabolic properties as TBZ, where its metabolites, like those of TBZ, bind to VMAT2, 5-HT7 and D2- receptors. The main advantage with this compound is that only one or two doses of dTBZ are needed daily instead of the three required for TBZ, due to its longer plasma half-life (3). The replacement of six hydrogen atoms with deuterium atoms in dTBZ leads to a different pharmacokinetic profile as deuterium-carbon bonds are stronger than hydrogen-carbon bonds, resulting in a more uniform systemic exposure (3, 50).

Valbenazine (VBZ) is a prodrug for the active metabolite (+)α-HTBZ, which is the same as for TBZ, and is selective for VMAT2. Differently to the other metabolites of TBZ, the second metabolite of VBZ does not affect other monoamine transporters or receptors. One dose daily is also sufficient for VBZ as (+)αHTBZ has a half-life of 16 to 23 hours (3)

1.3.3.3 Other known VMAT2 inhibitors

The psychostimulative effect of the drugs amphetamine, methamphetamine and cocaine are caused by increased DA in the synaptic cleft, either by affecting DAT or VMAT2 (49, 52). The VMAT2 inhibitor lobeline has shown selective inhibition of amphetamine effects by reducing DA output caused by amphetamine (52, 53). The selective, potent VMAT2 inhibitor GZ-11608 reduces DA release caused by methamphetamine from isolated synaptic vesicles from brain dopaminergic neurons. GZ-11610, an enantiomer of GZ-11608, is another VMAT2 inhibitor that inhibits locomotor activity induced by methamphetamine intake (54).

Ketanserin is a 5-HT antagonist that also inhibits VMAT2 and decreases aggression in monoamine oxidase A deficient mouse together with TBZ, without sedation (55). Compared to TBZ, ketanserin only shows moderate affinity for VMAT2 (52, 55). Lobeline does not inhibit the extracellular DA effects of methamphetamine (56), and is not selective for VMAT2 (52). GZ-11608 decreases the effect of methamphetamine, and has good efficacy, but has low bioavailability. GZ-11610 has issues with potency and efficacy, but is a good basis for the development of better compounds (54). The chemical structures of the aforementioned VMAT2 inhibitors are illustrated in Figure 1.7

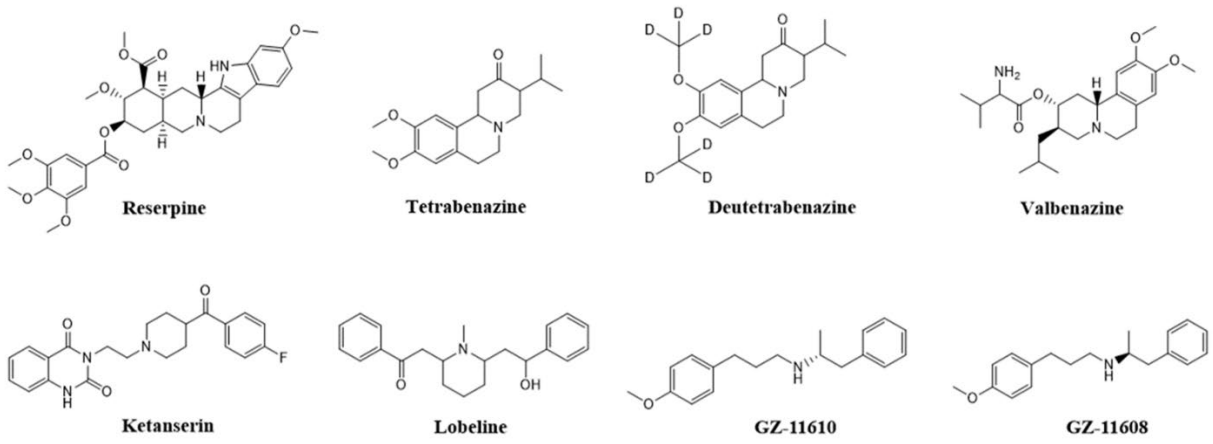

Figure 1.7: ***The molecular structure of known VMAT2 inhibitors.***

1.4 Screening

When screening for modulators of proteins, there are several different approaches that can be used, all with advantages and disadvantages. *In silico* or virtual screening allows screening of millions of compounds in a relatively short time. However, this method requires a high-resolution structural model of the protein and preferably, a known modulator binding site. All hit compounds further require thorough experimental validation. For many proteins, such as VMAT2, there are no available high-resolution structural models, making virtual screening difficult.

Biophysical screening is another approach based on purified proteins or biomolecules. Biophysical screens often monitor direct interactions either using techniques such as surface plasmon resonance or thermal stabilization by, for instance, differential scanning fluorimetry. Biophysical screening approaches can be very efficient for "well-behaving" proteins which are easy to purify, but can be more difficult and expensive for proteins such as membrane transporters that can be difficult to purify in high quantities.

A third approach is known as cell-based screening. Unlike target-based biophysical screenings that require protein purification, in cellular screening the protein-of-interest is expressed in cells by transfection. As the assay is done in cells, the target is in more similar physiological conditions found *in vivo* as compared to biophysical assays where purified proteins are typically suspended in buffer. Apart from this, cellular screening enables the analysis of increased protein levels across the proteome, the monitoring of phenotypic changes in the cell or the investigation of a direct functional effect, such as, for instance, the effect of compounds on substrate uptake.

Traditionally VMAT2 activity is studied experimentally in cells or when reconstituted in liposomes with radiolabelled VMAT2 substrates and due to the reactivity of DA [^{3}H] serotonin has been typically used for these experiments (19). Recently, however, the fluorescent VMAT substrate fluorescent false neurotransmitter 206 (FFN206) was developed, which is a non-radiolabelled VMAT substrate optimized for intact cell systems in cultures transfected with VMAT2. In fact, the signal-to-background ratio for FFN206 is higher for VMAT-transfected human embryonic kidney (HEK)-cells compared to untransfected HEK-cells (57). This synthetic substrate has a similar

structure to the monoamines transported by VMAT2, illustrated in Figure 1.8A, and enables high throughput screening (HTS).

Thus, for this project, we developed a cellular screening pipeline (Figure 1.8B) using FFN206 that has higher throughput than traditional cellular screening assays that use radiolabelled substrates, to measure inhibition or activation of VMAT2 using a microplate reader that quantifies VMAT2 activity.

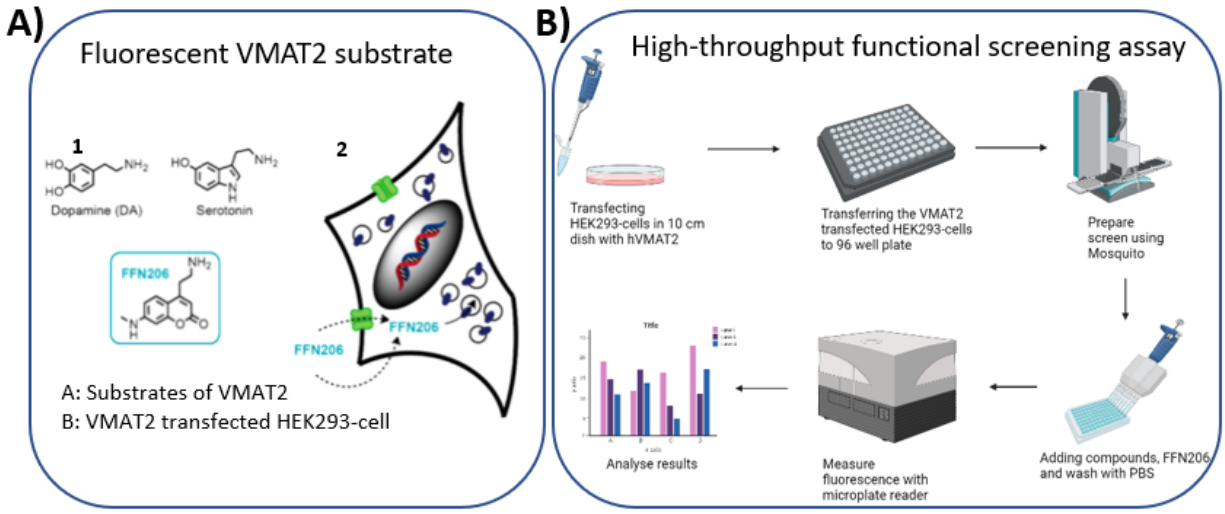

Figure 1.8: ***Overview of the high throughput functional screening assay, and how the fluorescent substrate is being accumulated by VMAT2.*** *A1: The structure of the VMAT2 substrate FFN206, and two monoamine neurotransmitters transported into synaptic vesicles by VMAT2 in neurons. A2: A HEK293-cell transfected with VMAT2, FFN206 being transported into vesicles by VMAT2. B: The workflow of the high-throughput functional screening assay used to screen the Prestwick chemical library ®. A: Is modified from (57) B:Created with Biorender.com.*

2 Aims of the project

Due to its role in the packaging of monoamines into synaptic vesicles, VMAT2 can function as an important regulator of monoamine homeostasis. Inhibition of VMAT2 leads to reduction of DA and other monoamine signalling into the synaptic cleft and has a therapeutic potential for symptomatic treatment of involuntarily movements disorders such as tardive dyskinesia and chorea associated with Huntington's disease. Activation of VMAT2 on the other hand will increase packing of monoamines such as DA into synaptic vesicles, and increase monoamine signalling into the synaptic cleft, having a therapeutic potential against PD.

Today a few VMAT2 inhibitors are approved for chorea associated with Huntington's disease and tardive dyskinesia, and there is an ongoing effort to further develop VMAT2 inhibitors for use in treatment of tardive dyskinesia (58). The use of activators of VMAT2 on the other hand has been suggested as a potential treatment of PD symptoms, but so far no VMAT2 activator has been identified (59).

In this project we thus aimed to:

1. To establish a cellular screening assay for VMAT2 using transfected HEK293 cells and a fluorescent VMAT2 substrate.
2. To use this screening assay to identify new modulators of VMAT2 function by screening among already approved drugs for repurposing.

By using a functional screening assay in cells the ultimate objective of the project is to identify both activators and inhibitors of VMAT2, as both of which have a potential role as therapeutics in monoamine disorders.

3 Materials and Methods

3.1 Materials

Chemical	Supplier
(+)-Isoproterenol (+)-bitartrate salt	Prestwick chemical library /greenpharma
^{3}H Salmeterol	Vitrax Radiochemicals
^{3}H Dihydrotetrabenazine	Vitrax Radiochemicals
Agar-agar	Merck
Ampicillin	Sigma Aldrich
Benzamil	Tocris
Benzonase®	Merck
Big-Dye 3.1	MGM Sequencing facility at HUS
Blocking Reagent	Qiagen
Blocking reagent buffer	Qiagen
c0mplete Tablets, mini EDTA-free, EASY pack	Roche
CaCl2	Merck
Calcium chloride dihydrate	Merck
Prestwick chemical library®	Prestwick chemical libraries
Dimethyl sulfoxide (DMSO)	Sigma Aldrich
DL-Dithiothreitol (DTT)	Sigma Aldrich
DMEM (high glucose)	Sigma Aldrich
DMEM (high glucose)	BioWest
Doxazosin mesylate	Prestwick chemical libraries /greenpharma
Enhancer - (p-Coumaric acid)	Sigma Aldrich
Fetal bovine serum	Sigma Aldrich
FFN206-dihydrochlorid	Tocris
Gatifloxacin	Prestwick chemical libraries /greenpharma
Geneticin	Gibco
Glucose	Sigma Aldrich
Glycerol	Sigma Aldrich
Glycine	Sigma Aldrich

H_2O_2	Merck
KCl	Sigma Aldrich
Luria-Bertani broth	Lennox
L-Glutamin	Sigma Aldrich
Lippfectamine™ LTX	Invitrogen
Luminol (3-Aminophthalhydrazide, 5-Amino-2,3-dihydro-1,4-phthalazinedione)	Sigma Aldrich
Methanol	Sigma Aldrich
MgCl2 + 6*H2O	Merck
MgSO4	Sigma Aldrich
MiniPrep monarch	New england biolabs
NaCl	Merck
Opti-MEM™	Gibco™
Penicillin/streptomycin	Sigma Aldrich
Penta-his-hrp-conjugate	Qiagen
Pepton	Merck
Phosphate buffered saline (PBS)	Sigma Aldrich
Plasmids	GenScript
PLUS™ reagent	Thermo Fischer Scientific
Precision Plus Dual color standard	Bio Rad
Prenylamine lactate	Prestwick chemical libraries /greenpharma
SDS 20%	Sigma Aldrich
Sequence buffer	MGM Sequencing facility at HUS
Tetrabenazine	Cayman chemical company
Thioperamide	Tocris
Trimebutine	Prestwick chemical libraries /greenpharma
Trizma base	Sigma Aldrich
Trypsin-EDTA solution	Sigma Aldrich
Tween 20	Sigma Aldrich
Ultima Gold	Perkin Elmer
Yeast extract	Sigma Aldrich

Table 3.1: List of plasmids used for expression of tagged human VMAT2 (hVMAT2), human VMAT2 with green fluorescent protein (hVMAT2-GFP) and human VMAT1 (hVMAT1), their tag and their antibiotic resistance.

Plasmids	Antibiotic resistance	Tag
pcDNA3.1 hVMAT2-GFP-His	Ampicillin, neomycin, kanamycin, geneticin	His
pcDNA3.1 hVMAT2-His	Ampicillin, neomycin, kanamycin, geneticin	His
pcDNA3.1 hVMAT1-His	Ampicillin, neomycin, kanamycin, geneticin	His

3.2 Preparation of VMAT2-expressing cells

3.2.1 Heat shock transformation

To prepare plasmids for transfection, expression and cellular screening of human VMATs (hVMATs) we first had to prepare large amounts of pcDNA3.1 plasmids containing the open reading frames (ORFs) of hVMAT1 and hVMAT2. The plasmids in Table 3.1, with illustrated plasmid maps in Figure 3.1 were transformed into *E. coli* XL10-gold competent cells by heat shock transformation. Briefly, 100 µL of XL-10 gold cells was thawed on ice and divided in two, where 50 µL was used for control and 50 µL was used for transformation. Next, 0.250 µg of plasmid was added and mixed by stirring with pipette tip to ensure mixing, followed by incubation on ice for 20-30 min. Then, the cells were heat shocked for 40 seconds at 42 ℃ to ensure DNA uptake, before being placed immediately on ice for 2 min. The transformed cells were then supplemented with 750 µL of super optimal broth with catabolic repression (SOC) media and mixed by turning the tube prior to incubation at 37 ℃ without agitation for 35 - 45 minutes. 20 µL and 100 µL of the transformed cells were plated out on agar plates containing 100 µg/ml ampicillin, before being placed upside down at 37 ℃ overnight.

A single cell colony was transferred from one plate and added to 7.5 - 10 ml Luria-Bertani (LB) broth with 100 µg/ml ampicillin in a 50 mL Falcon tube and incubated overnight in a shaking incubator (180 RPM) at 30 or 37 ℃. This was done for each plate containing a different plasmid.

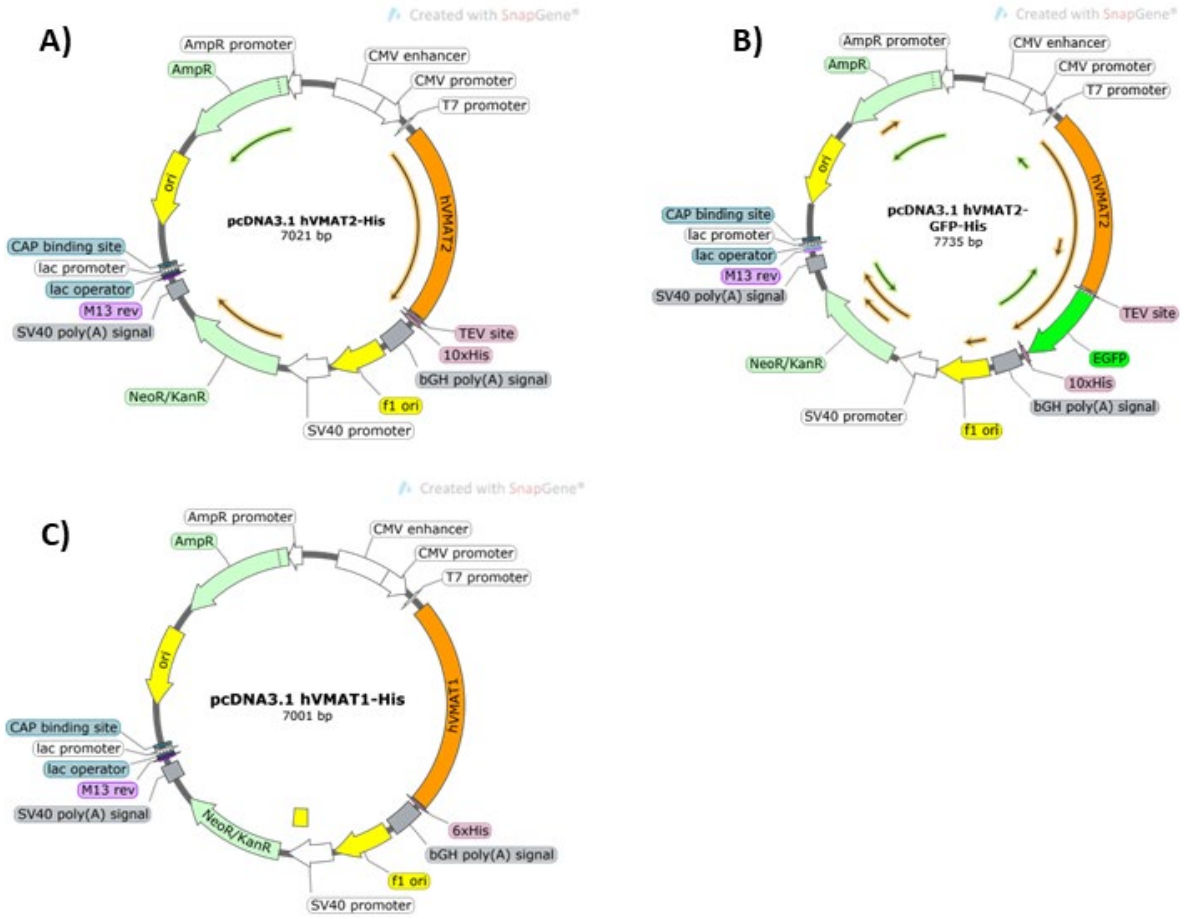

Figure 3.1: ***Maps of used plasmids.*** *A) pcDNA3.1 hVMAT2-His, B) pcDNA3.1 hVMAT2—GFP-His,* and *C) pcDNA3.1 hVMAT1-His. Plasmid maps show among other the antibiotic resistance, the ORFs of human VMAT1 (hVMAT1) and VMAT2 (hVMAT2) with fusion tags and promotors, in addition to other features. From: SnapGene software (Insightful Science).*

3.2.2 Plasmid purification

To isolate and purify the DNA from section 3.2.1, a plasmid MiniPrep kit from New England Biolabs was used according to the manufacturer's protocol. In brief, pellets were resuspended in 400 µL of plasmid resuspension buffer, 400 µL of lysis buffer was added to disrupt the cells, before 800 µL of plasmid neutralization buffer was added to neutralize the lysis solution. The lysate was centrifuged at 13 000 x g with miniSpin (Eppendorf) for 5 min to remove cell debris, and the supernatant transferred to spin columns for binding of DNA. Spin columns were washed and plasmids eluted in elution buffer in 1.5 ml Eppendorf tubes. The DNA concentration was measured with NanoDrop One© (Thermo Scientific).

3.2.3 Sequencing

All purified plasmids were sequenced for verification using the standard Big-Dye version 3.1 protocol for sample preparation. Primers used are listed in Table 3.2 and the DNA sequencing mix is listed in Table 3.3. A polymerase chain reaction (PCR) was run with the program in Table 3.4, before the samples were submitted to MGM Sequencing facility at Haukeland University hospital for sequencing.

Table 3.2: Sequencing primers

Primer	Sequence
T7PetF	TAATACGACTCACTATAGGG
hVMAT2_FWD_seq_362	CGACTGTCCCAGTGAAGAC
hVMAT2_FWD_seq_918	CATCTGCTTTGCAAACATG
hVMAT2_FWD_seq_1416	TCTGCTTTTTTCTTCGAAGTC
hVMAT2_FWD_seq_918	CATCTGCTTTGCAAACATG

Table 3.3 Components of PCR mix

Components	Amounts
Big-Dye version 3.1	1 µL
Sequencing buffer	1 µL
Template	200 ng
Primer	3.2 pmol
Deionised water	Quantum satis
Total volume	10 µL

Table 3.4: Cycling parameters for PCR

Step	Temperature °C	Time	Cycles
Initial denaturation	96	5 min	1
Denaturation	96	10 s	25
Annealing	50	5 s	
Elongation	60	4 min	
Hold	4	∞	1

3.3 Cell culture

3.3.1 HEK293 cells

HEK293 are versatile cells which are easy to transfect, enabling expression of proteins in cellular conditions to study their function (60). The HEK293 cells were cultivated in Dulbecco's Modified Eagle Medium (DMEM) - High glucose (4500 mg/L) and sodium bicarbonate supplemented with 10% fetal bovine serum (FBS), 2 mM L-glutamine and 1% penicillin-streptomycin (10 000 U/mL penicillin and 10 mg streptomycin/mL).

The cells were cultured in 10 cm dishes to 90 % confluency and passaged regularly to maintain the cells, approximately 3 times a week. For passaging, cells were detached using Trypsin-EDTA solution and resuspended in a 1:10 or 1:20 dilution in warmed growth medium. Cells were grown in a cell incubator at appropriate conditions of 37 °C, 5% CO_2. The cells were handled in a laminar air flow (LAF) bench maintain sterile conditions during experiments and procedures.

3.3.2 Transfection with Lipofectamine™ LTX and PLUS™ Reagent

To perform experiments on VMAT1 and VMAT2 in HEK293 cells, we transfected and transiently expressed hVMAT2-His, hVMAT2-GFP-His or hVMAT1-His. hVMAT2-GFP-His was used for optimization of transfection and expression protocols. Optimization parameters included the amount of plasmid and transfection reagents, whether the cells should be transfected in Opti-MEM™ or in DMEM supplemented with 10% FBS and 2mM L-glutamine with and without 1% penicillin-streptomycin (10 000 U/ml penicillin and 10 mg streptomycin/ml) and with and without 250 µg/ml geneticin. The transfection parameters were assessed by evaluating the amount of transfected cells (expressing hVMAT2-GFP-His) in a fluorescence microscope, eclipse TS100 (Nikon). The amounts of plasmid and transfection reagents are listed in Table (3.5)

Table 3.5: Optimized transfection protocol

	Solution A			Solution B	
	DNA	Opti-MEM™	Plus™ Reagent	Lipofectamine™ LTX	Opti-MEM™
24 well dish	0.5 µg	25 µL	1 µL	2 µL	25 µL
10 cm dish	15 µg	750 µL	30 µL	60 µL	750 µL

For high-throughput screening, cells were transfected at a confluency of approximately 80-90%. Before transfection the old medium was exchanged with fresh DMEM medium supplemented with FBS and L-glutamine without antibiotics. For the transfection in a 10 cm dish 15 µg of plasmid DNA were diluted in 750 µL Opti-MEM™, before 30 µL of room temperature PLUS™ Reagent were gently mixed and added, and incubated for 5 min at room temperature. In a different tube 60 µL of room temperature Lipofectamine LTX reagent were diluted in 750 µL Opti-MEM™ and mixed, before added to the diluted DNA and mixed, then incubated for 5-10 min. The solution was added dropwise to the cells.

3.4 Uptake assay

To verify that the high throughput functional assay would detect VMAT2 substrate uptake, and subsequently inhibitors of VMAT2 by detecting a reduction in the measured activity, HEK293 cells transfected with hVMAT2, hVMAT2-GFP and untransfected HEK293 cell controls grown in a 96 well plate coated with Poly-D-Lysine (Corning, BioCat) were preincubated in 50 µL of Opti-MEM™ either without the VMAT2 inhibitor TBZ, or TBZ at a final concentration of 100 nM and 1 µM at 37 °C for 20 min, before the substrate uptake assay was started by adding 50 µL Opti-MEM™ with 10 µM (5 µM final concentration) of the fluorescent VMAT2 substrate FFN206 at 37 °C for 20 min. Uptake assays were stopped by washing cells 3 x 10 min with 70 µL PBS before adding 100 µL of PBS prior to measuring fluorescence in all wells with Tecan Spark 20M (Bergman Diagnostika) plate reader. The measured fluorescence in the untransfected HEK293 control cells was subtracted from the measured fluorescence in the transfected HEK293 cells.

3.5 High throughput functional screening

3.5.1 High throughput functional screening assay

For the high-throughput functional screening assay, HEK293 cells were transfected in 10 cm dishes as described in section 3.3.2 and transferred to 96 well plates coated with Poly-D-Lysine (Corning, BioCat) one day after transfection. Typically, one confluent 10 cm dish was distributed to two 96 well plates in 100 µL growth medium per well. The high throughput functional screening assays were performed the following day (day two after transfection).

For the setup of screening, stock solution for the assay of the compounds were prepared using the mosquito ® HV (TTP LabTech) pipetting robot, diluting the compounds and controls in phosphate buffered saline (PBS) and transferring compounds into a 96 well plate (Greiner). Columns 2 – 11 of the 96 well plates contain 80 different compounds, column 1 is the negative control (DMSO), representing the expected activity for compounds not affecting VMAT2 and column 12, positive control, contains TBZ, representing fully inhibited VMAT2 in the same concentration as the screened compounds.

Firstly, old medium was removed from the wells, followed by preincubation of the cells with 45 µL/well of PBS with compounds from Prestwick compound library® for 20 min at 37 °C. The final concentration of compounds in the uptake assay was 5 µM or 1 µM (preincubation with 45 µL/well of 2x stock 10 µM or 2 µM compound in PBS). After preincubation, the uptake assay was initiated by addition of 45 µL of Opti-MEM™ with the fluorescent VMAT2 substrate FFN206 at a final concentration of 5 µM for 20 min at 37 °C. The uptake assay was stopped by washing cells with 70µL/well PBS 3 times at room temperature, before 100 µL/well PBS was added for quantification of fluorescence in the plate reader. For measurement the Tecan spark 20M (Bergman Diagnostika) was used, with an excitation and emission wavelengths of 369 nm and 464 nm, respectively, with multiple reads distributed in a 4 x 4 grid around in the well.

To analyse the results, the average of the measured activity in the positive control for each 96 well plate, were subtracted from the activity in the other wells. A screening hit was defined as activity

measured to be either higher (potential activator) or lower (potential inhibitor) than the hit threshold, defined as the average activity in the negative control, plus/minus 3x standard deviations (STD) of all negative controls in both the 1 µM and 5 µM plates.

3.6 Structural clustering

To analyse which compounds were similar in chemical structure, we performed a molecular clustering of hits from the initial screening, using Schrodinger Canvas (Schrödinger Release 2020-1: Maestro, Schrödinger, LLC, New York, NY, 2020). All initial hit compounds and TBZ were selected and binary fingerprints that could be used for among other hierarchical clustering were created based on the 2D structure of all compounds. Clustering was performed using the hierarchical clustering option in Schrodinger Canvas.

3.7 Validation of hits from screening

The initial screening threshold yielded a large number of hit compounds that affected VMAT2 activity. To reduce the number of hit compounds for validation, we increased the threshold to 5 x STD of DMSO controls in at least one of the tested concentrations (1 µM or 5 µM). As there was room for three extra compounds on the final validation plates some compounds not fulfilling the inclusion criterium were chosen for further validation. Hit compounds from the screening were validated by assessing inhibition or activation at four different concentrations, 5 µM, 1 µM, 0,200 µM and 0,04 µM using the same protocol for the validation assay as were used in the high-throughput screening of the library (see section 3.5.1).

TBZ were used as a positive control with the same concentration as the tested compounds, the average activity of the 5 µM positive control was subtracted from the activity of the other wells, representing full inhibition. To normalize the activity of each 96 well plate, the activity of all wells was divided by the average measured fluorescence of the negative control containing DMSO. To determine which compounds should be further analysed, the validation of the hits was performed by a dose-response assay. To reduce the number of hits after validation, the hit threshold was set to 5 x STD of the negative control (DMSO) for three or four out of four concentrations, using the same concentration for DMSO and the compound.

3.7.1 IC50 and EC50 of compounds

The half-maximal inhibitory concentration (IC_{50}) is the concentration of a compound necessary to obtain 50% inhibition of a reaction or process. The half-maximal effective concentration (EC_{50}) on the other hand is the concentration of a compound necessary to obtain 50% of maximal response of the compound.

For the most promising compounds from validation experiments, we determined EC_{50} and IC_{50} values towards both VMAT1 and VMAT2. Cells were incubated with compounds at concentrations ranging from 0 to 270 µM, using 12 different concentrations. Each experiment was performed in four replicates, also including four replicates of untransfected control cells at each concentration for subtraction of background fluorescence. The IC_{50} and EC_{50} experiments were performed with the same protocol as was used in the high-throughput functional assay, using the listed conditions and concentrations, see section 3.5.1.

To calculate the IC_{50} and EC_{50} values, the background fluorescence activity of the untransfected control cells for each column with one concentration were subtracted from the measured activity of the transfected cells for the same concentration. After subtraction, normalisation was performed by dividing the activity of the average of the parallels at 0 µM. The IC_{50} values were calculated using nonlinear fit, [inhibitor] vs. response – Variable slope (four parameters) in GraphPad Prism 9.3.1. The EC_{50} values were calculated using the same method, but using [agonist] vs. response instead.

3.7.2 Inhibitor displacement assay

As an indirect approach to study VMAT2 binding, and to further validate any effects of the most promising hit compounds, we performed an inhibitor displacement assay with two radiolabelled VMAT2 inhibitors, [^{3}H] dihydrotetrabenazine (HTBZ) and [^{3}H] salmeterol. HEK293 cells were transfected as described in section 3.3.2 with hVMAT2 in 10 cm dishes, grown for two days, before harvesting the cells in ice cold PBS using a scraper and pelleting the harvested cells using a

Centrifuge 5810 R (Eppendorf) at 2361 g, flash freezing cells in liquid nitrogen, and stored at – 80 ℃ until the day of the experiment.

The cells were lysed by thawing and resuspending the pellet in 700 µL or 1600 µL PBS with 1 x protease inhibitor and dounce homogenized in a 1ml dounce homogenizer, before transferring 20 µL of lysate to each well of a 96 well plate. 10 µL of 50 µM compound diluted in PBS and a DMSO control was added to four wells with transfected cells, and four wells of non-transfected HEK293 cells for each compound. The homogenized cell samples were preincubated with compounds at a final concentration of 50 µM in 96 well plates at 37 ℃ for 20 min, before 20 µL, 2 nM (final) [^{3}H] TBZ was added to each well, followed by incubation for 20 min at 37 ℃. The second time 10 µL of 50 µM compound diluted in PBS was added to eight wells of hVMAT2-transfected HEK293 cells and preincubated for 20 min at 37 ℃, followed by addition of 2 nM [^{3}H] HTBZ to four wells for each compound, and the last four wells were incubated with 15 nM [^{3}H] salmeterol for 20 min at 37 ℃. A DMSO control and non-transfected HEK293 cells were added to four wells for [^{3}H] HTBZ and [^{3}H] salmeterol each.

After the last incubation, the treated lysates were transferred to MulitScreen®FB, Opaque plates (1.0 µm Glass Fiber type B Filter, Millipore), and the assay was stopped by quickly spinning down the reaction mix through the filter plate in a Centrifuge 5810 R (Eppendorf) and the filter plates were washed twice with 100 µL PBS and spun down between each time. 40 µL of Ultima-Gold scintillation cocktail was added to each well and incubated for 20 min - 16 h per plate before measuring emission using MicroBeta2 (Perkin Elmer).

3.7.3 Autofluorescence testing of thioperamide

Thioperamide was among the hit compounds that were validated by concentration dependent validation and selected for further IC_{50} and EC_{50} analysis. Upon determination of EC_{50} values however it quickly became evident that thioperamide had similar effects on both transfected HEK293 cells as well as untransfected control cells. Autofluorescence properties were examined by diluting thioperamide in PBS and examining autofluorescence in a Tecan Spark 20M (Bergman Diagnostika) plate reader, using the same parameters as in the screening assay. Further, a series of

experiments were performed as described in the Results section (4.7). HEK293 cells were cultured, transfected and transferred to the 96 well plate coated with Poly-D-Lysine (Corning, BioCat) as described in section 3.3, 3.5 and 3.7.1. Substrate uptake assays were performed where different parameters were examined. Substrate uptake was assayed in the presence and absence of the fluorescent VMAT substrate FFN206 to verify that the increased fluorescence observed with increasing concentrations of thioperamide was not due to compound autofluorescence. Five different concentrations of thioperamide and a control (ranging from 0 - 30 μM) were analysed either with or without adding FFN206. Assays were also performed in the presence and absence of TBZ to examine the effects of inhibition of VMAT2 on the increased fluorescence. Again, five different concentrations of thioperamide and a control (0 - 30 μM) were analysed, either with or without pre-treatment with 200 nM TBZ.

3.8 Sodium dodecyl sulphate polyacrylamide gel electrophoresis (SDS-PAGE)

SDS-PAGE separates the proteins by their molecular weight. To verify the presence of VMAT2 in our samples we dissolved a small aliquot of cells in PBS supplemented with the endonuclease benzonase to reduce viscosity in the sample, followed by sonication (Elma Ultrasonic bath Transonic T 310) for one minute (230 V. 50/60 Hz. 150 mA. 35 kHz). The samples were diluted in 2x loading buffer (SB) (100 mM Tris-HCl, 0.2 % (w/v) bromophenol blue, pH 6.8, 20% (v/v) glycerol with 4 % (w/v) SDS and 100 mM DTT immediately added prior to use), followed by heating for 30 min at 42 °C. The cell lysate was loaded on a 4-15% Mini-PROTEAN®TGX™ Precast gel (Bio-Rad), with Precision Plus™ Dual Color Standard (Bio-Rad) as a ladder. The gel was run at 180 V until dye reached the end of the gel, using 1X SDS-running buffer (25 mM Tris, 192 mM glycine, 0.1% SDS, pH 8.3).

3.9 Western blot

To detect the presence of VMAT2 in the transfected HEK293 cells, western blot was performed. Western blot is a method enabling detection of specific proteins, in a mixture of several proteins. To identify the specific protein in the sample, the membrane is first blocked with blocking buffer to prevent unspecific binding, followed by incubation with an anti-his-HRP-conjugate (Qiagen) binding to the his-tag of the target protein.

The gel from the SDS-PAGE (section 3.8) was transferred onto a nitrocellulose membrane using the Trans-Blot®-Turbo™ Transfer pack (Bio-Rad) and the Trans-Blot®-Turbo™ Transfer system (Bio-Rad) (Turbo, 1 mini gel, mixed Mw, 1.3A, 25V, 7 min). The membrane was washed twice for 10 min with PBS, before being incubated 1 h with blocking reagent buffer. Next the membrane was washed twice for 10 min with PBS containing Tween-20 (0.1%) (PBS-T), followed by a 10-min wash with PBS. The membrane was then incubated overnight at 4 °C with Anti-His-HRP conjugate solution (1/2000), dissolved in blocking reagent buffer. The membrane was washed twice for 10 min with PBS-T, and then washed once for 10 min with PBS. Chemiluminescent detection was performed by using ECL enhancer (198 µM final), luminol (1.439 mM final) and H_2O_2 (0.01% final) diluted in Tris (0.1 M, pH 8.5), and incubated on membrane for 1 min before imaging with Chemidoc XRS+ (Bio-Rad).

4 Results

4.1 Screening preparation

In order to perform a functional screening of VMAT2 we used the fluorescent VMAT substrate FFN206 which is taken up by cells and packed into vesicles or membranous compartments by both VMAT1 and VMAT2. FFN206 can be used for the HTS thanks to its optimization for intact cell systems, enabling measurement of VMAT2 activity in cells by a microplate reader (57). We chose transiently transfected HEK293 cells for our studies as these are mammalian cells with the post-translational system necessary for expression of membrane proteins (61), are easy to transfect and maintain (62), and have acidic vesicles suited for expression of - and substrate uptake assays with - proton coupled membrane transporters such as VMAT (57). They also provide vacuolar H^+-ATPase, generating the proton gradient used by VMAT2 to transport substrates into vesicles (57), as well as neuronal properties, which is useful when studying neuronal proteins (61). FFN206 provides a high signal-to background ratio for VMAT2 transfected HEK293 cells compared to non-transfected HEK293 cells (57), which is utilised by having non-transfected HEK293 cells as the control for the determination of IC_{50} and EC_{50}.

4.1.1 Expression of VMAT2 in transfected HEK293 cells

Prior to screening, VMAT2 transfection of HEK293 cells was optimized to identify the ideal conditions for transfection and expression of VMAT2, and to reduce the amount of DNA and transfection reagent needed without reducing the transfection effectivity (data not shown). The optimized transfection protocol was used for all subsequent transfections of HEK293 cells in 10 cm dishes (see description in the method section 3.3.2). The day after transfection, cells were transferred to 96 well plates coated with Poly-D-Lysine. The Poly-D-Lysine coating enhances attachment of the cells, which was a great advantage due to the large amount of washing steps in the substrate uptake protocol.

To investigate VMAT2 expression in the transfected HEK293 cells, we collected cell samples, lysed them, and analysed the cell lysate by SDS-PAGE and western blotting (Figure 4.1A). As can be seen in Figure 4.1A HEK293 cells transfected with either hVMAT2-his or hVMAT2-GFP-His

express VMAT2, while no expression is detected in non-transfected HEK293 control cells. In lane 1 there is band slightly above 50 kDa, corresponding well with the theoretical size of hVMAT2 of 56 kDa. In lane 2 there is a band at approximately 75 kDa, corresponding well with the theoretical size of hVMAT2-GFP of 83 kDa. In addition, there is a stronger band at approximately 30 kDa, corresponding with theoretical weight of free GFP of 27 kDa.

We also examined hVMAT2-GFP expression in HEK293 cells 2 days after transfection in a fluorescence microscope. As seen in Figure 4.1 B 1) hVMAT2-GFP transfected cells, clearly had GFP expression, while surrounding cells not expressing hVMAT2-GFP had no fluorescence. In Figure 4.1 B 2), a picture of the same area of well is taken by light microscopy, demonstrating that not all cells express hVMAT2-GFP after transfection.

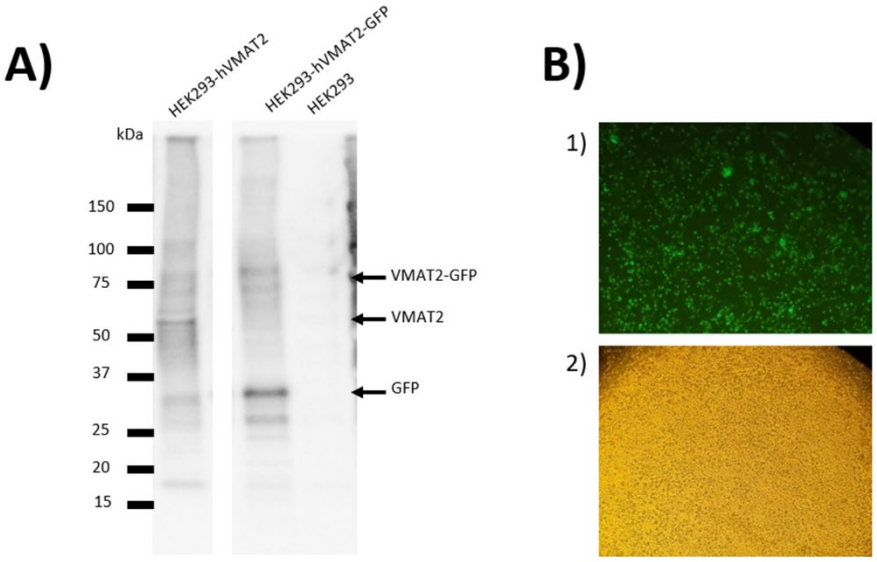

Figure 4.1: ***Expression of hVMAT2 and hVMAT2-GFP in HEK293 cells.*** *A) Western blot using anti-his HRP antibody showing the presence of hVMAT2-His and hVMAT2-GFP-His in transfected HEK293 cells. Non-transfected HEK293 cells is used as control. The band at approximately 50 kDA in lane 1 shows hVMAT2. The bands in lane 2 at approximately 80 kDa show hVMAT2-GFP-His, while the band at approximately 30 kDA shows free GFP-His. B) HEK293 cells transfected with hVMAT2-GFP-His in fluorescence microscope. In picture 1) the bright green cells are HEK293 cells expressing hVMAT2-GFP-His. In picture 2), the same area of the well taken with light microscopy showing the confluency of the cells. The pictures were taken using a camera through the microscope lens.*

4.1.2 Uptake test assay

To verify that HEK293 cells transfected with VMAT2 would accumulate the fluorescent substrate FFN206, an initial substrate uptake test assay was performed. FFN206 uptake was measured in transfected HEK293 cells in the absence and presence of the VMAT2 inhibitor TBZ to verify that substrate accumulation could be inhibited by the VMAT2 specific inhibitors. Non-transfected HEK293 cells were used as controls and unspecific FFN206 uptake measured from control cells were subtracted from the signal measured in transfected HEK293 cells. As can be seen in Figure 4.2, the activity is highest with no inhibitor present (PBS control), and the activity decreases with increasing concentration of TBZ. This demonstrates that inhibition of transfected HEK293 cells with VMAT2 inhibitors reduces the measured substrate uptake activity and that the approach can be used further for screening of new VMAT2 modulators.

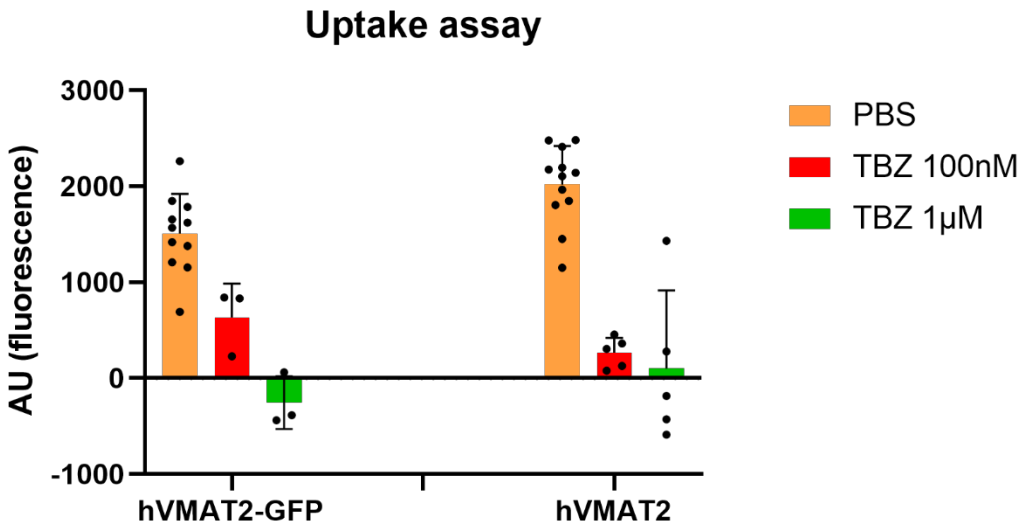

Figure 4.2: ***Uptake assay in HEK293-cells transfected with hVMAT2 or hVMAT2-GFP****. Illustrating that inhibition of VMAT2 reduces uptake of the fluorescent VMAT2 substrate FFN206. Statistical significance was tested with one-way ANOVA test using GraphPad Prism 9.3.1. Inhibition with TBZ leads to a statistically significant (one way ANOVA) reduction of substrate uptake for both hVMAT2-GFP and hVMAT2. p-values: PBS vs TBZ 100 nM for hVMAT2-GFP: $p<0.05$, PBS vs 1 µM TBZ for hVMAT2-GFP $p<0.0001$ and PBS vs both TBZ 100 nM and TBZ 1 µM for hVMAT2: $p<0.0001$.*

4.2 Screening of Prestwick Chemical library®

After we had optimized settings for protein expression and protocols for the substrate uptake assay, we screened 1280 compounds of the Prestwick chemical library®, monitoring VMAT2 activity by this assay. The library consists mainly of U.S Food and Drug Administration (FDA) approved drugs, but also European Medicines Agency (EMA) approved drugs. These drugs have a known bioavailability, pharmacological diversity and are off-patent. Already approved, bioavailable off-patent drugs may give a shorter way from research to drug repurposing. The screening assay was performed two days after transfection, in 96 well plates, with 80 different compounds in each plate. The remaining 16 wells were controls, 8 positive controls (effect: VMAT2 inhibitor TBZ) and eight negative controls (no effect: DMSO). The medium was removed from the cells prior to addition of compounds in PBS which was incubated for 20 min at 37 ℃. Next FFN206 in Opti-MEM™ was added, followed by incubation for 20 min at 37 ℃. After incubation, the plates were washed three times with PBS, followed by measurement with microplate reader.

To reduce the number of false hits the library was screened at two concentrations of compounds, 1 and 5 µM. Hit compounds were defined as the compounds causing an increase or decrease of VMAT2 activity that where larger than 3 x the standard deviation (STD) of the DMSO negative controls. In Figure 4.3, the positive and negative controls, and the compounds and hit thresholds are illustrated. The initial screening of 1280 compounds from the Prestwick Chemical library® gave 55 hits, listed in Table 4.1.

An example of a set of 80 compounds screened in 96 well plates at both 1 and 5 µM concentrations is shown in Figure 4.3. The example of initial results illustrates the difference in number of hits at both concentrations for the same compounds. Each bar represents one well in the 96 well plate, were controls, hits, test compounds and possible inhibitor and activator hits have their own colour. To remove background fluorescence from all measurements, the average activity of the positive control (inhibition with TBZ) representing fully inhibited VMAT2, was subtracted from all activity measurements.

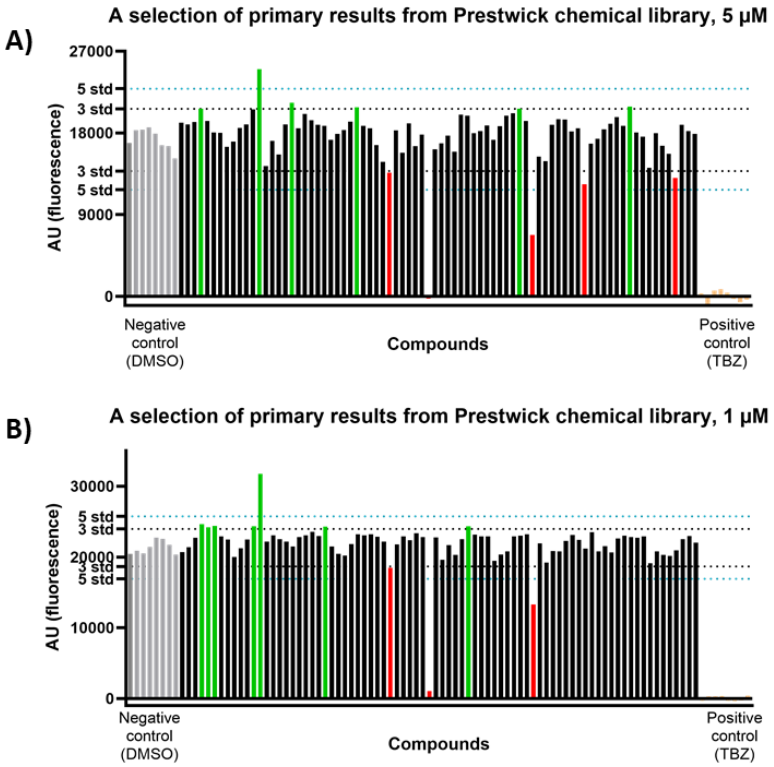

Figure 4.3: ***Example of initial results in 2 plates from screening, with the same compounds from the Prestwick Chemical library®, at 5 µM and 1 µM respectively****. Green bars are potential activators and red bars are potential inhibitors. Black bars represent compounds in the library, with in total 80 different compounds. Grey bars are negative controls, transfected HEK293 cells treated with DMSO. Orange bars are positive controls, hVMAT2 transfected HEK293 cells inhibited with the potent VMAT2 inhibitor tetrabenazine (TBZ). For visulaization, the average of the positive control were subtracted from all values, representing fully inhibitied of VMAT2. Hit thresholds of 3x STD of DMSO controls are shown as grey stippled lines and 5x STD of DMSO as blue stippled lines. Hits were selected based on the selected hit threshold.*

Table 4.1: List of hits from the screening of Prestwick Chemical library®. The compounds were tested on hVMAT2 transfected HEK293 cells. All hits identified in both the 1 µM and 5 µM screening dataset, using 3x STD of DMSO controls as a hit threshold. The cluster number is based on the clustering of the hits performed using Scrödinger Canvas where compounds are clustered together based on similarity. Numbers correspond to clusters in Figure 4.4. Pw-number is the number of the compound in the Prestwick chemical library ®. The "Discovered by DSF" column includes the common hits found in a target-based screening by differential scanning fluorimetry (DSF) with purified VMAT2 and using the same library (63). The therapeutic effect is provided with the Prestwick chemical library®.

Cluster	Prestw-nr	Chemical name	Therapautic effect	Discovered by DSF (63)	Activator (A) / inhibitor (I)
1	Prestw-434	Cefadroxil	Antibacterial		I
2	Prestw-832	Cefoxitin sodium salt	Antibacterial		I
3	Prestw-880	Carbachol	Antihypertensive		A
4	Prestw-331	Tremorine dihydrochloride	CNS Stimulant		A
5	Prestw-78	Thioridazine hydrochloride	Antipsychotic	**X**	I
5	Prestw-529	Mesoridazine besylate	Antipsychotic		A
6	Prestw-74	Amitryptiline hydrochloride	Antidepressant		I
6	Prestw-488	Dosulepin hydrochloride	Antidepressant		I
7	Prestw-1290	Imatinib	Antineoplastic		I
8	Prestw-1188	Ziprasidone Hydrochloride	Antipsychotic	**X**	I
9	Prestw-858	Doxazosin mesylate	Antihypertensive		I

9	Prestw-947	Prazosin hydrochloride	Antihypertensive		I
10	Prestw-499	Propafenone hydrochloride	Antiarrhythmic	**X**	I
10	Prestw-1262	Carvedilol	Antihypertensive	**X**	I
11	Prestw-76	Dibucaine	Local anesthetic		I
11	Prestw-630	Dimethisoquin hydrochloride	Antipruritic		I
12	Prestw-310	Mebeverine hydrochloride	Antispastic		I
12	Prestw-380	Clebopride maleate	Antiemetic		I
12	Prestw-559	DO 897/99	Antidepressant		I
12	Prestw-704	Bromopride	Antiemetic		A
12	Prestw-831	Butacaine	Anesthetic		I
12	Prestw-1777	Trimebutine	Antispastic		I
13	Prestw-1514	Darifenacin hydrobromide	Not provided		I
14	Prestw-277	Labetalol hydrochloride	Antihypotensive	**X**	I
14	Prestw-911	(+)-Isoproterenol (+)-bitartrate salt	Antiasthmatic		A
14	Prestw-945	Salmeterol	Bronchodilator	**X**	I
14	Prestw-974	Pronethalol hydrochloride	Antianginal	**X**	I
14	Prestw-1602	Indatraline hydrochloride	Antidepressant	**X**	I
15	Prestw-174	Alverine citrate salt	Antispastic		I
15	Prestw-270	Fendiline hydrochloride	Antianginal	**X**	I
15	Prestw-311	Ifenprodil tartrate	Vasodilator	**X**	I
15	Prestw-312	Flunarizine dihydrochloride	Anticonvulsant	**X**	I
15	Prestw-386	GBR 12909 dihydrochloride	Antidepressant	**X**	I
15	Prestw-560	Prenylamine lactate	Antianginal		I
15	Prestw-788	Hexylcaine hydrochloride	Anesthetic		I
16	Prestw-657	Benzamil hydrochloride	Antihypertensive		I
17	Prestw-144	Loperamide hydrochloride	Antidiarrheal	**X**	I
17	Prestw-392	Ketanserin tartrate hydrate	Antihypertensive	**X**	I
17	Prestw-484	Benperidol	Antipsychotic		I
17	Prestw-509	Bromperidol	Antipsychotic		I
17	Prestw-1117	Azaperone	Antipsychotic		I
18	Prestw-1130	Azelastine HCl	Antihistaminic	**X**	I
19	Prestw-922	Thioperamide maleate	Antiemetic		A
20	Prestw-1341	Sertindole	Antipsychotic		I
21	Prestw-318	Quinacrine dihydrochloride hydrate	Antihelmintic		I
21	Prestw-1284	Hydroxychloroquine sulfate	Antimalarial		A
22	Prestw-1760	Tegaserod maleate	Gastroprokinetic		I
23	Prestw-1510	Dolasetron mesilate	Antiemetic		I
24	Prestw-875	Reserpine	Antipsychotic	**X**	I
26	Prestw-1265	Gatifloxacin	Antibacterial		A
26	Prestw-1740	Besifloxacin hydrochloride	Antibacterial		A
27	Prestw-588	Galanthamine hydrobromide	Analgesic		I
28	Prestw-1441	Mevastatin	Hypocholesterolemic		I
29	Prestw-321	Streptomycin sulfate	Antibacterial		A
30	Prestw-676	Beta-Escin	Antineoplastic		I

The hits obtained from this screening were compared to the list of hits found by Støve et al (63) by using a target-based biophysical screening based on differential scanning fluorimetry (DSF), using purified VMAT2. DSF screening detects changes in the thermal melting temperature of a purified protein upon binding to small molecules (64). When comparing the results from the DSF screening, 16 of the 55 hits in the cellular screening (29.1%) had also been identified by DSF. As can be seen in Table 4.1, compounds identified in both screening projects include known VMAT2 inhibitors (ketanserin, reserpine) (63), dopamine antagonists (ziprasidone hydrochloride, thioridazine) (65, 66), histamine antagonist (azelastine) (67), antiarrhythmic (propafenone) (68), opioid agonist (loperamide) (69), calcium channel blocker (flunarizine) (70), N-methyl-D-aspartate receptor antagonist (ifenprodil) (71), non-selective monoamine transporter inhibitor (indatraline) (72), beta-adrenergic agonist (salmeterol) (73), and beta-antagonists (labetalol, carvedilol) (74, 75). The two compared screening methods apply very different assays to identify compound hits, as the screening by DSF is based on how compounds affect the stability of an isolated target protein while the screening presented in this work is based on how the compounds affect the function of the protein in a cellular environment. The large number of positive hits was therefore encouraging, but it was also interesting to observe how different screening methods can detect different sets of hit compounds.

To further examine our list of hit compounds, and to identify any structural similarities between them we performed a hierarchical clustering of all initial hit compounds based on their 2D structures using Schrodinger Canvas (Schrödinger Release 2020-1: Maestro, Schrödinger, LLC, New York, NY, 2020). As can be seen from Figure 4.4 several hit compounds clustered together suggesting similarity among the compounds. The closer to the bottom of the hierarchical tree two compounds diverge from each other, the higher similarity there is between the compounds. For illustrative purposes all compounds have been divided and coloured into 30 different structural clusters. An overview of clustered compounds can also be found in Table 4.1. The two compounds thioridazine and mesoridazine in cluster 5, the two compounds doxazosin and prazosin in cluster 9 and the two compounds gatifloxacin and besifloxacin in cluster 26 have the highest degree of similarity among each other. The chemical structures are illustrated in Figure 4.5, together with an example of a larger cluster (14) containing indatraline, a non-selective monoamine transporter inhibitor (72), together with the beta agonists salmeterol and (+)-isoproterenol (+)-bitartrate salt

(73, 76) and the beta antagonists labetalol, pronethalol (77, 78), where indatraline is the first compound to the right in the cluster, being the compound deviating the most from the other compounds in that cluster. The largest cluster is 15, among other containing the hit prenylamine lactate and the known VMAT2 inhibitor GBR12909 (12). Another large cluster is 12, containing the hit trimebutine used for irritable bowel syndrome (IBS) (79), so does another compound in the cluster, mebeverine hydrochloride (80). Other compounds in the same cluster are dopaminergic antagonist and local anaesthetics.

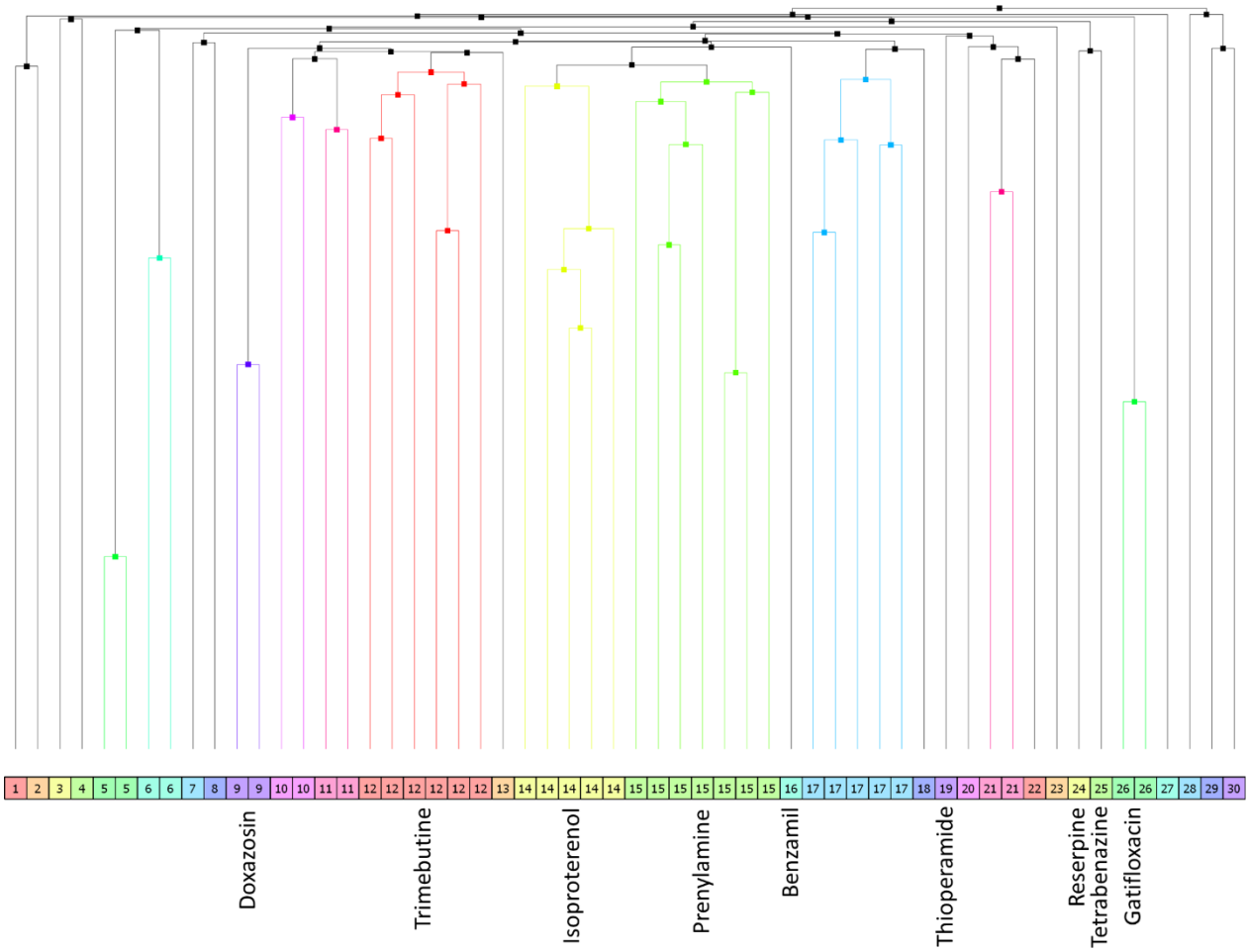

*Figure 4.4:**Clustering of all hits from the initial screening of Prestwick chemical library®.** The 7 hits selected for further evaluation is named, in addition the known VMAT2 inhibitors tetrabenazine and reserpine are labelled. Figure made with Schrodinger Canvas 2020-1.*

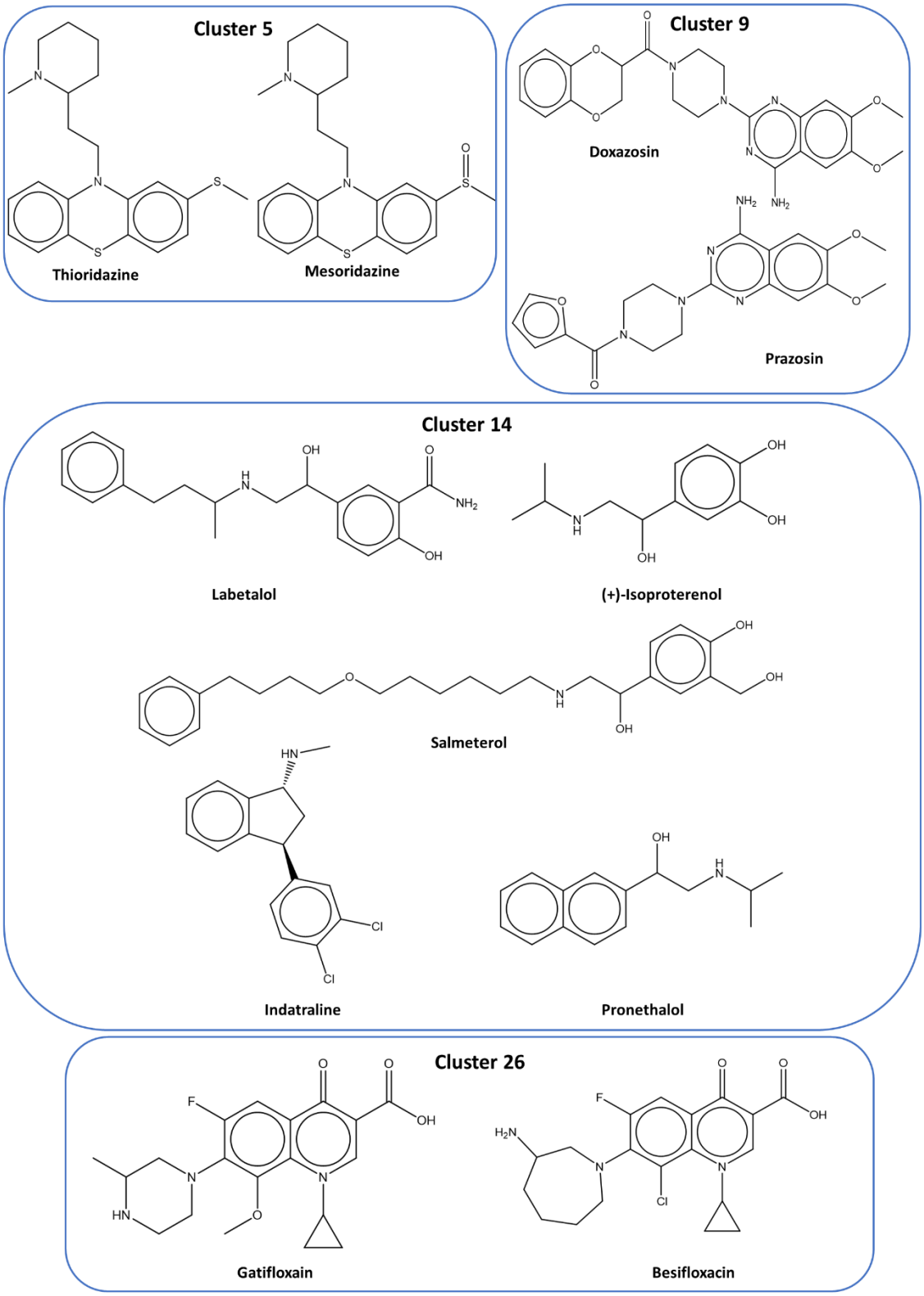

Figure 4.5: ***Illustration of molecular structures for selected clusters.*** *The chemical structure of selected hits in the clusters 5, 9, 14 and 26 is shown, to illustrate the similarities between compounds in each cluster. The compounds in clusters 5, 9 and 26 present highest similarity, while cluster 14 is one of the larger clusters.*

4.3 Validation of hits from the screening

To validate hit compounds, we selected 33 of the modulators found in the initial screening, which were tested in a concentration dependent manner. To narrow down the number of hits from the initial screening further, we increased the VMAT2 activity threshold so that compounds that had an increased or decreased uptake of fluorescent substrate FFN206, exceeding the 5x STD of DMSO controls at either 1 or 5 µM, were subjected to concentration dependent validation. An illustration of the hit thresholds and the difference between the 3 x STD and 5 x STD threshold is illustrated in Figure 4.3. Among the hits selected for validation, two hit compounds that fulfilled the criteria but that were already known VMAT2 inhibitors (reserpine and ketanserin) (5), were excluded from the validation assay. Due to extra space on the final 96 well validation plate, three extra hit compounds (two potential activators and one potential inhibitor) that did not fulfill the selected criteria were subjected to validation, and are included in the thesis.

In the validation assay 13 of the 33 tested compounds were validated as inhibiting or activating VMAT2 function more than the 5 x STD threshold, in the three highest concentrations tested (5, 1 and 0.2 µM) (Figure 4.6). Among those 13, five were potentially activating compounds, and eight were potentially inhibiting compounds. Of those eight, salmeterol is a known inhibitor (63). Four compounds were not outside 5 STD for any concentration during the validation, while other fulfilled the criteria for one or two concentrations. (+)-Isoproterenol (+)-bitartrate salt were chosen for further analysis, because even though their effect on the VMAT2 activity was only greater than 5 x STD for one concentration, they presented higher uptake than most compounds at this one concentration (Figure 4.6). The results for the remaining 20 compounds can be found in appendix, Figure 9.2.

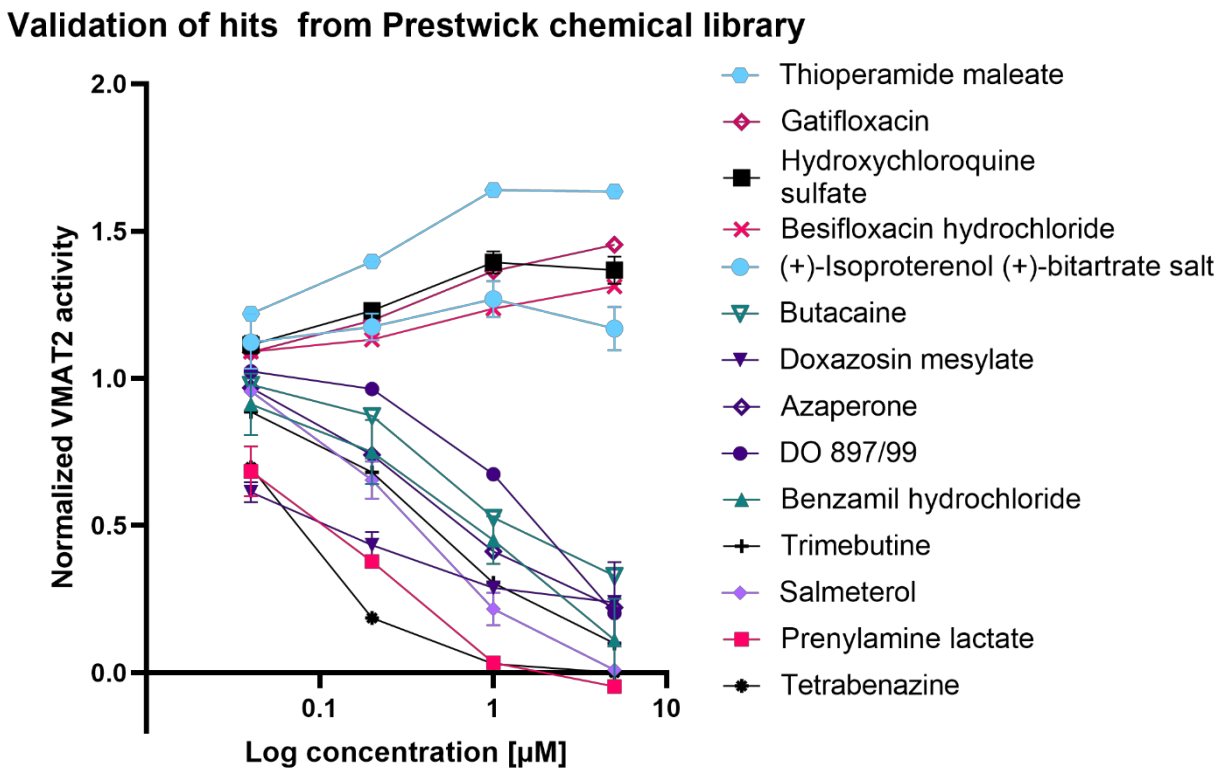

Figure 4.6: ***The most promising hits from the validation assay, either activating or inhibiting VMAT2.*** *The top five curves are five activating compounds, and the bottom eight are inhibiting compounds. Tetrabenazine and salmeterol are already known potent VMAT2 inhibitors.*

Out of the 13 compounds fulfilling the criteria for being a hit in the concentration dependent validation assay, seven were further analysed to determine IC_{50} and EC_{50}. The hits not selected for further analysis are besifloxacin, salmeterol, hydroxychloroquine, butacaine, DO 897/99 and azaperone. Besifloxacin has a very similar structure to gatifloxacin (Figure 4.5), and they clustered as two of the most similar compounds among all hits (Figure 4.4). Choosing both of these would most likely be redundant, and thus gatifloxacin was chosen for further analysis as the apparent VMAT2 activation was higher compared to besifloxacin in the validation experiment. Salmeterol is a known VMAT2 inhibitor, and was therefore not selected for further analysis (63). Hydroxychloroquine is an indirect known VMAT2 modulator, affecting the proton gradient used by VMAT2 for transport of substrates by de-acidifying the vesicles (81). Butacaine was the least inhibiting modulator of VMAT2 among the validated hits and is a local anaesthetic (82) that disturbs inhibitory neuronal depolarisation in CNS (83), and therefore butacaine is not likely suitable for drug repurposing for VMAT2. Finally, DO 897/99 a DA agonist for which a clinical

trial in United Kingdom for cocaine abuse was discontinued (84), and the antipsychotic azaperone, a DA antagonist (85) that is only used in veterinary medicine as a sedative for pigs (86). Due to this, DO 897/99 and azaperone were not very interesting for drug repurposing and were not subjected to further analysis. The chemical structure of all the selected compounds together with the known VMAT2 inhibitor TBZ are illustrated in Figure 4.7. The compounds are then listed with their therapeutical class in Table 4.2.

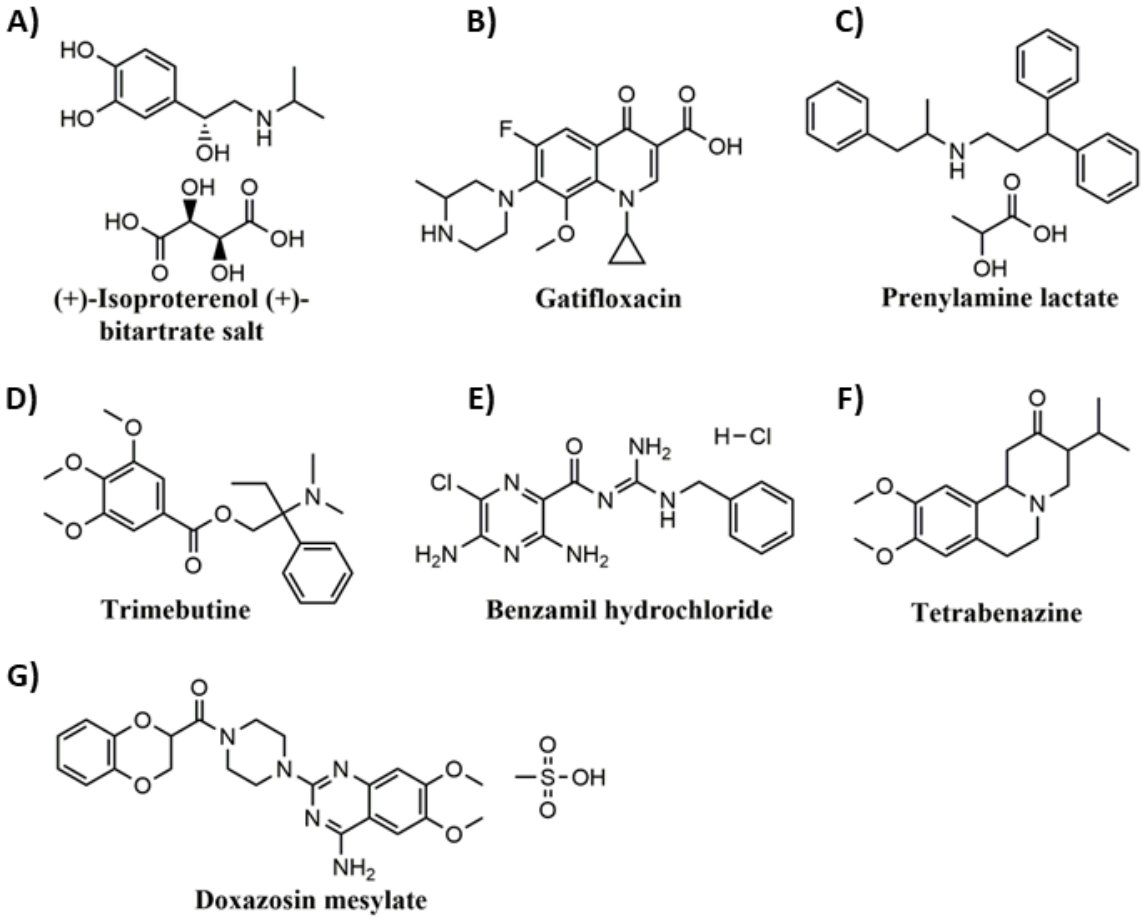

Figure 4.7: ***Chemical structures the hit compounds chosen for further evaluation and of tetrabenazine, a known VMAT2 inhibitor.*** *A-E, G: Chemical structures of all the compounds chosen for further evaluation after the concentration dependent validation assay. F) Tetrabenazine.*

Table 4.2: List of therapeutic properties for the compounds to further evaluation after the validation assay, and the known VMAT2 inhibitor tetrabenazine. The information about therapeutic class is from information provided with the Prestwick chemical library®.

Compound	Therapeutic class	Subtype of therapeutic class
(+)-Isoproterenol (+)-bitartrate salt	Respiratory	β-adrenergic receptor agonist(76)
Gatifloxacin	Infectiology	Bacterial DNA gyrase and topoisomerase IV inhibitor (87)
Prenylamine lactate	Cardiovascular	Calcium channel blocker (88)
Trimebutine	Neuromuscular	Antimuscarinic (79)
Benzamil hydrochloride	Metabolism	Epithelial sodium channel blocker (89)
Tetrabenazine	-	VMAT2-inhibitor (1)
Doxazosin mesylate	Cardiovascular	Alfa-1a-adrenergic antagonist (90)

A schematic overview of the screening process and selection of hits from the functional screening is provided in Figure 4.8.

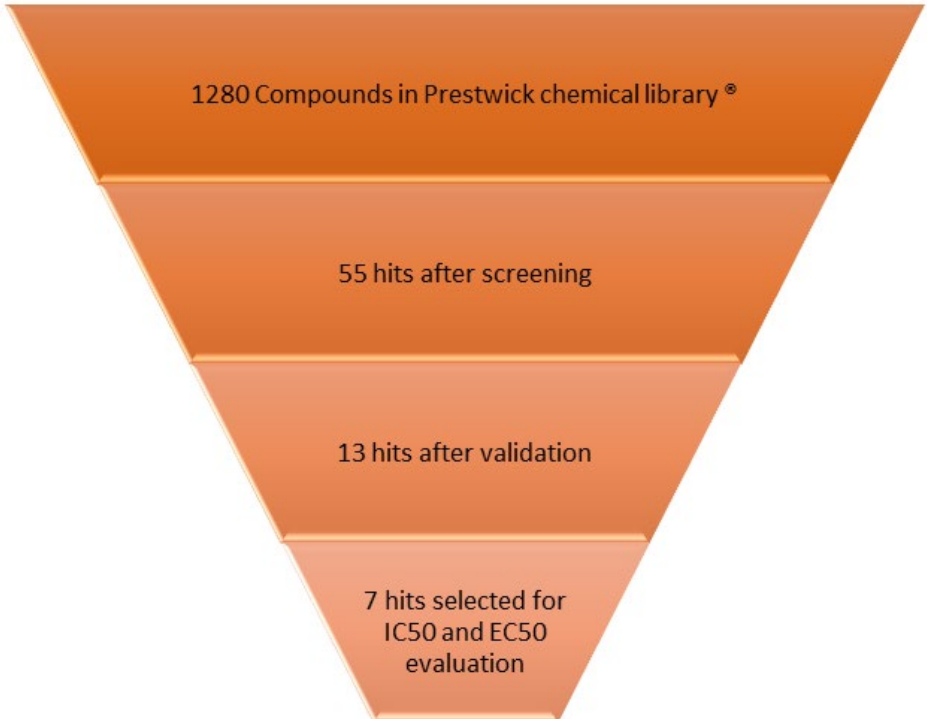

Figure 4.8: **From 1280 Prestwick compounds to 7 promising VMAT2 modulators.** The screened library contains 1280 compounds, from which 55 were hits after the initial screening with two different concentrations. Next, a concentration dependent validation was performed to reduce the hits for further evaluation. After the validation 13 compounds fulfilled the criteria, where some were already known inhibitors and some were not chosen to further evaluate for other reasons, ending up with seven compounds for further evaluation.

4.4 IC_{50} and EC_{50} for VMAT2

Next, we wanted to determine the potency of the most promising VMAT2 modulators from the validation assay by establishing IC_{50} and EC_{50} values. All experiments were performed at least 3 times. For compounds where the IC_{50} or EC_{50} had varying values between the initial three repetitions, additional experiments were performed. The average IC_{50} and EC_{50} value for each compound is listed in Tables 4.3 and 4.4. In Figure 9.3 in appendix, all IC_{50} and EC_{50} curves for each compound are shown, while a selection is also presented in Figure 4.9A-F.

Prenylamine lactate is the most promising inhibitor of the compounds evaluated, being the inhibitor with the lowest IC_{50} value, followed by trimebutine and benzamil. Neither of these compounds however have as low IC_{50} as TBZ, a potent VMAT2 inhibitor. The IC_{50} curves for these compounds are shown in Figure 4.9. The conclusion based on the IC_{50} curves for each compound and their derived IC_{50} values is that they inhibit VMAT2 to varying extent. The IC_{50} value for doxazosin mesylate could not be obtained due to large variation of signal both in transfected cells and in the non-transfected control cells, and in between experiments. While for trimebutine and benzamil IC_{50}-values of 0.205 μM and 0.759 μM, respectively, could be calculated. For the potential activators, gatifloxacin demonstrates a weak increase in activity, as shown in Figure 4.9 B, while the curve for (+)-isoproterenol (+)-bitartrate salt is near flat (Figure 4.9 A). The EC_{50} values should therefore be interpreted with caution for these two, especially for (+)-isoproterenol (+)-bitrate due to the substandard fitting of the curve giving an inaccurate EC_{50} value. Therefore, one cannot conclude that (+)-isoproterenol (+)-bitartrate salt and gatifloxacin activate VMAT2, only that they potentially can activate.

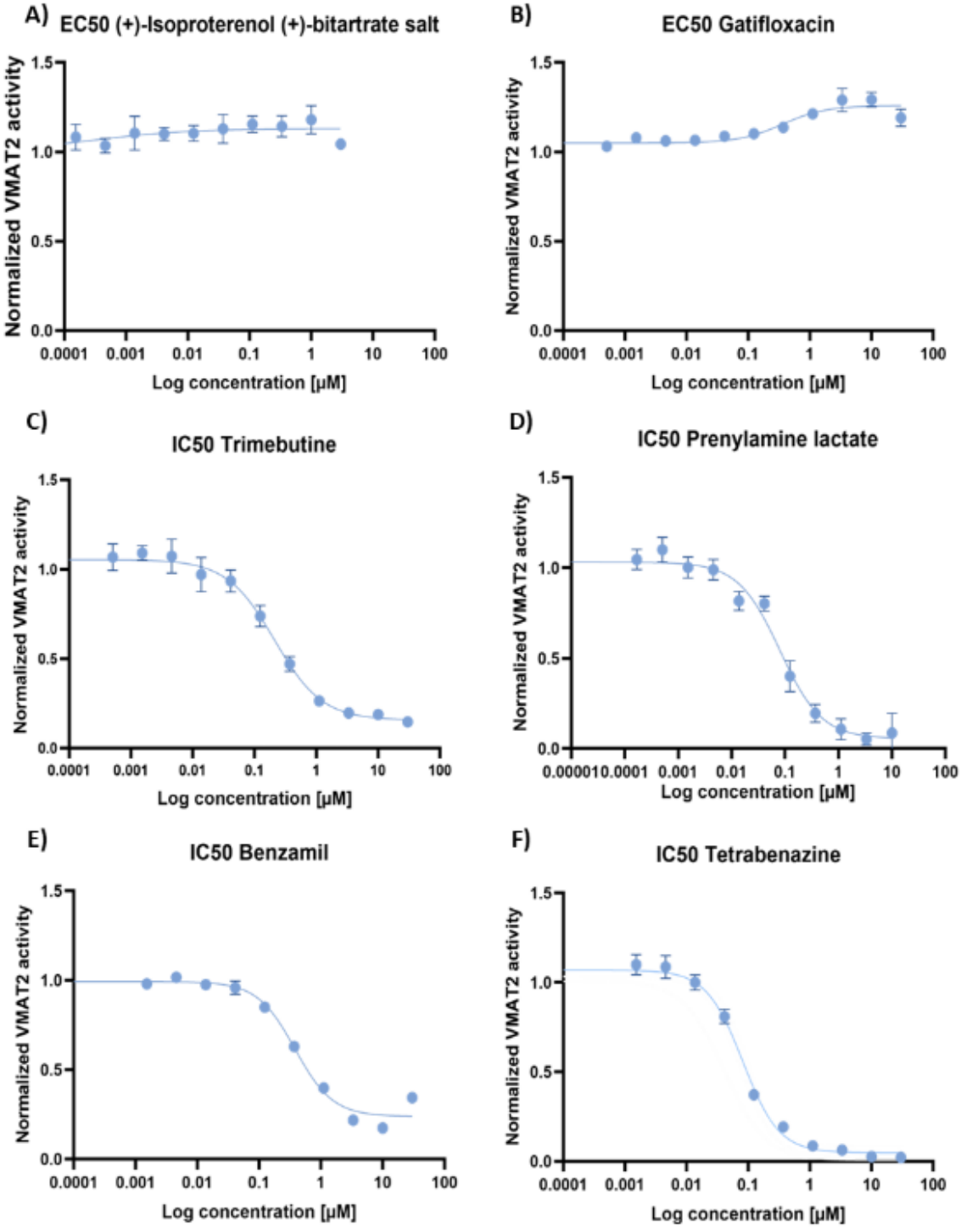

Figure 4.9: ***EC_{50} and IC_{50} curves for VMAT2****. A) (+)-isoproterenol (+)-bitartrate salt, B) gatifloxacin, C) trimebutine, D) prenylamine lactate, E) benzamil and F) tetrabenazine. One representative curve is shown for each compound, illustrating the level of activation or inhibition of VMAT2.*

Table 4.3: EC_{50}-values of potential activator hits for VMAT2, with the number of repetitions for each compound. The EC_{50} value is the average of the obtained EC_{50} values from each repetition.

Compound	Repetitions	EC_{50} (µM)
(+)-Isoproterenol (+)-bitartrate salt	7	0.032 ± 0.001
Gatifloxacin	6	0.450 ± 0.427

Table 4.4: IC_{50}-values of hits for inhibitors of VMAT2, with the number of repetitions for each compound. The IC_{50} value is the average of the obtained IC_{50} values from each repetition.

Compound	Repetitions	IC_{50} (µM)
Trimebutine	6	0.205 ± 0.155
Prenylamine lactate	3	0.124 ± 0.047
Benzamil	4	0.759 ± 0.406
Doxazosin mesylate	5	Could not be deduced
Tetrabenazine	3	0.072 ± 0.023

4.5 Inhibitor displacement assay

Next, we were interested in examining whether hit compounds could bind directly to VMAT2 and compete with the VMAT2 inhibitors [^{3}H] dihydrotetrabenazine ([^{3}H] HTBZ) and [^{3}H] salmeterol. Cell lysates were preincubated with 50 µM compounds for 20 min at 37 °C before 2 nM [^{3}H] HTBZ and 15 nM [^{3}H] salmeterol were added and the mixture incubated for 20 min at 37 °C. As can be seen in Figure 4.10, preincubation of the inhibitory compounds prenylamine lactate and doxazosin mesylate reduced [^{3}H] HTBZ and [^{3}H] salmeterol binding by approximately >90% and 70%, respectively, while benzamil reduced binding by approximately 50% at the compound concentration we tested. The fourth inhibitor we tested, trimebutine, did not alter [^{3}H] HTBZ or [^{3}H] salmeterol binding and neither did any of the two potential activating compounds (gatifloxacin and (+)-isoproterenol (+)-bitartrate).

Altogether these results indicate that prenylamine, doxazosin and benzamil bind directly to VMAT2 in a manner that can compete with both [^{3}H] HTBZ and [^{3}H] salmeterol binding. The results need to be treated with caution however, and additional experiments with a more direct

assay to measure VMAT2 compound binding should be performed. Although there was a lack of effect on [^{3}H] HTBZ and [^{3}H] salmeterol binding for trimebutine, gatifloxacin and (+)-isoproterenol (+)-bitartrate, they might still directly interact with VMAT2, for instance either with lower affinity or in a different binding site of VMAT2 that does not affect ^{3}H] HTBZ and [^{3}H] salmeterol binding. VMAT2 activators might have a different binding site than inhibitors, which we cannot detect with this assay. To gather more information about the affinity, IC_{50} and EC_{50} experiments could be performed using [^{3}H] HTBZ and [^{3}H] salmeterol.

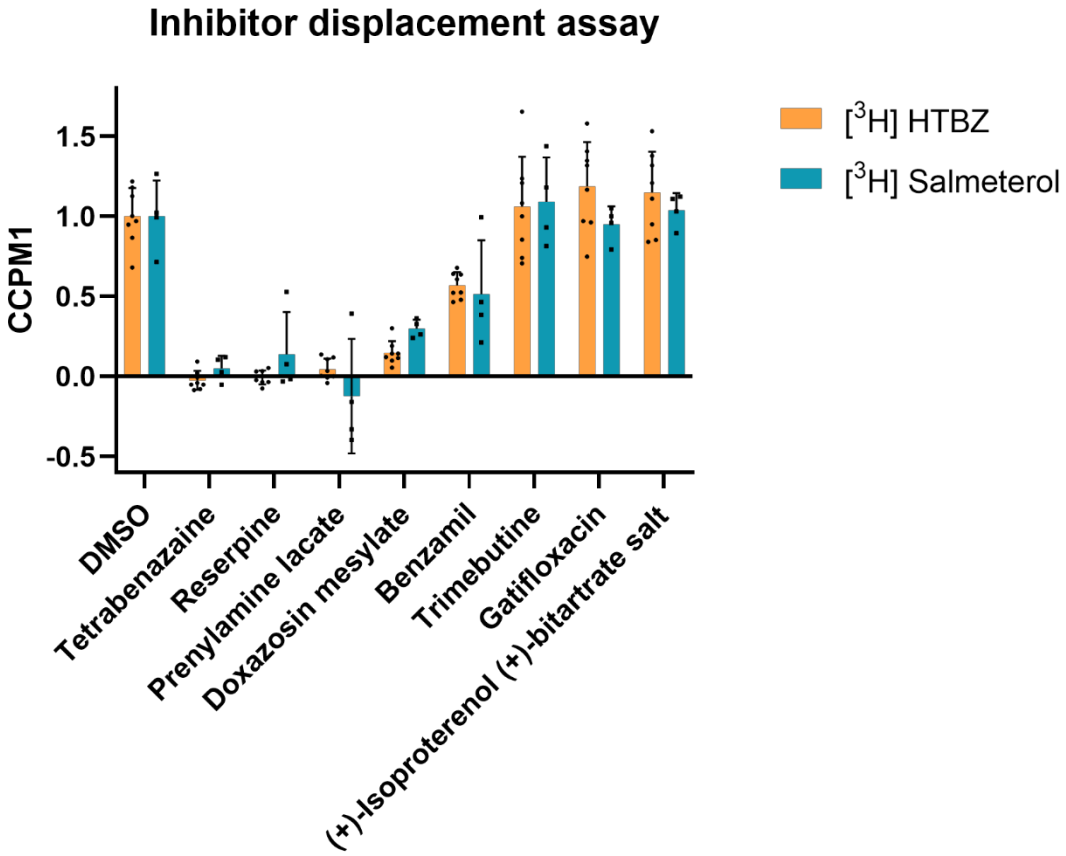

Figure 4.10: ***Inhibitor displacement assay between hit compounds and [^{3}H] HTBZ and [^{3}H] salmeterol.*** *HTBZ and salmeterol are known VMAT2 inhibitors. DMSO is the negative control. Low CCPM1 means that the compound competes with [^{3}H] HTBZ and/or [^{3}H] salmeterol, which indicates that the compound directly binds to VMAT2 at the same location as [^{3}H] HTBZ and [^{3}H] salmeterol or induces a conformational change which makes [3H] HTBZ and [^{3}H] salmeterol unable to bind to VMAT2. Statistical analysis were performed using one-way ANOVA in GraphPad prism. The reduction in [^{3}H] dihydrotetrabenazine and [^{3}H] salmeterol binding observed for tetrabenazine, reserpine, prenylamine and doxazosin are all statistically significantly compared to the DMSO control ($p<0.001$), while the reduction observed for benzamil is statistically significant compared to the DMSO control ($p<0.05$).*

4.6 Inhibition of VMAT1

Lower target specificity for drugs can lead to more side effects. VMAT2 is mainly located in CNS, while VMAT1 is in PNS (3). Modulators affecting VMAT1 as well as VMAT2 have therefore the potential for producing more peripheral side effects than those who do not affect VMAT1, and VMAT2 specific modulators are thus preferred. TBZ is a specific VMAT2 inhibitor, and with a much lower affinity for VMAT1 than for VMAT2 (4).

The validated compounds were analysed to check if they specifically modulated VMAT2 activity or if they also affect VMAT1 by determining their IC_{50} and EC_{50} value towards VMAT1. Comparing the IC_{50} values for VMAT2 and VMAT1, listed in Table 4.6, the determined IC_{50} values are generally higher for VMAT1 than for VMAT2, but the differences are not statically significant (one-way ANOVA calculated in GraphPad Prism 9.3.1). For benzamil, an IC50 value against VMAT1 could not be deduced. The highest concentration used for IC50 determination of benzamil towards VMAT1 was 270 µM, which was not high enough to get a flattening of the curve, and an accurately determined IC_{50} value. Even though the curve did not flatten out, making it difficult to obtain an IC_{50} value, the IC_{50} value for benzamil for VMAT1 would be notably higher than for VMAT2. This suggest that benzamil, although not as potent as prenylamine and trimebutine, might have a high specificity for VMAT2 over VMAT1, and highlights benzamil as a good starting point for further drug derivatization aimed at developing new specific VMAT2 inhibitors.

The EC_{50} values obtained for gatifloxacin are on the contrary lower for VMAT1 than for VMAT2 (Table 4.5), although the activating effect is small, and the EC50 calculations uncertain. For (+)-isoproterenol (+)-bitartrate salt, lower concentrations increased VMAT2 substrate uptake while the highest concentrations gave an inhibitory effect, and the datapoints for the two and three highest concentrations are removed from the curve for the calculation of EC_{50}. The full curves are shown in appendix, Figure 9.4, and a representative curve for each compound is shown in Figure 4.11.

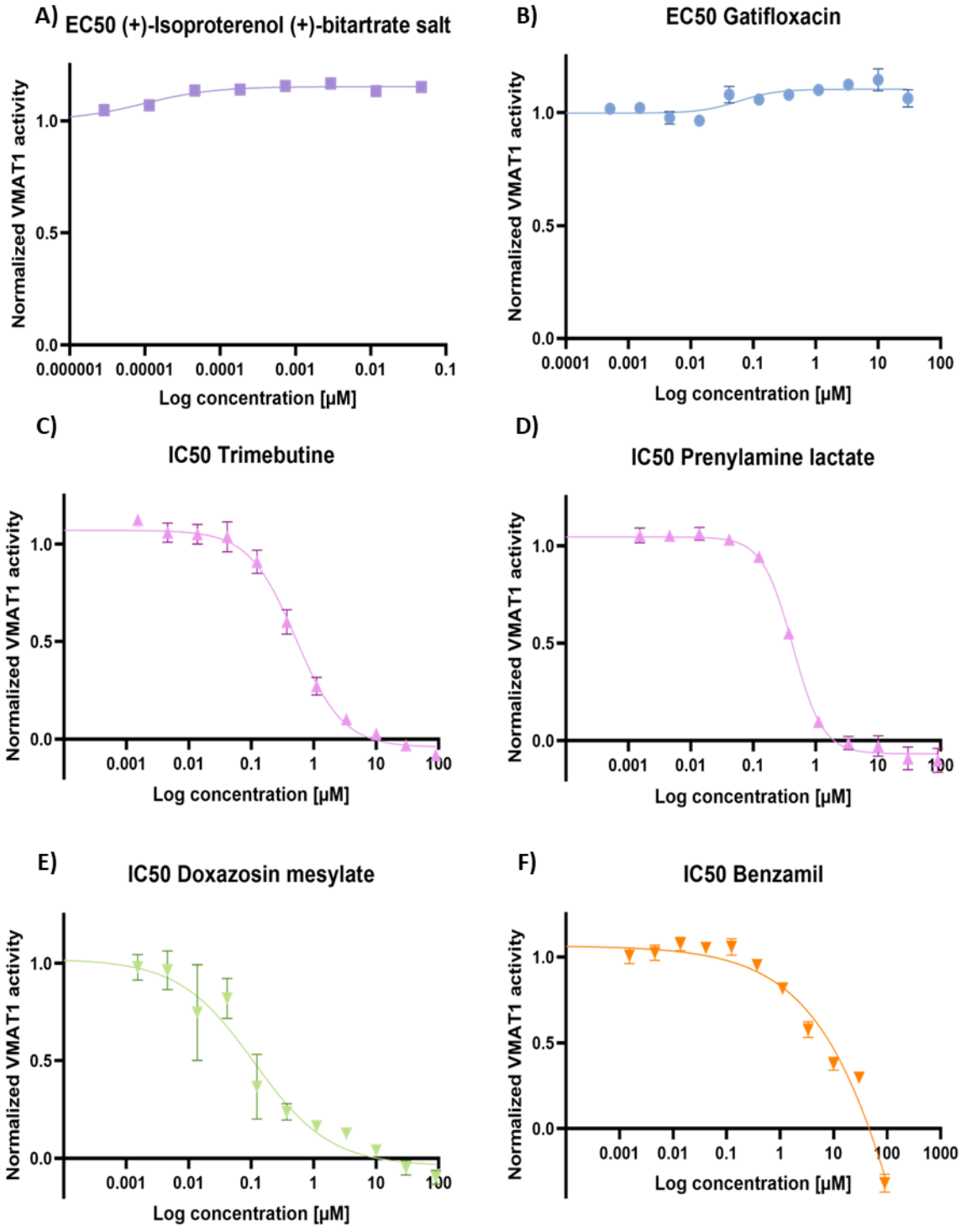

Figure 4.11: ***IC_{50} and EC_{50} curves for VMAT1.*** *A) (+)-isoproterenol (+)-bitartrate salt, B) gatifloxacin, C) trimebutine, D) prenylamine lactate, E) doxazosin mesylate and F) benzamil. One representative curve is shown for each compound, illustrating the level of activation or inhibition.*

*Table 4.5: EC_{50} of hits for VMAT1 and VMAT2. The EC_{50} value is the average of the obtained EC_{50} values from each repetition for VMAT1. * The same values are shown in Table 4.3.*

Compound	Repetitions	EC_{50} (µM) for VMAT1	EC_{50} (µM) for VMAT2*
(+)-Isoproterenol (+)-bitartrate salt	2	Could not be deduced	0.032 ± 0.001
Gatifloxacin	3	0.125 ± 0.106	0.450 ± 0.427

*Table 4.6: IC_{50} of hits for VMAT1 and VMAT2. TheIC_{50} value is the average of the obtained IC_{50} values from each repetition for VMAT1. * The same values are shown in Table 4.4.*

Compound	Repetitions	IC_{50} (µM) for VMAT1	IC_{50} (µM) for VMAT2*
Trimebutine	4	0.411 ± 0.232	0.205 ± 0.155
Prenylamine lactate	4	0.417 ± 0.201	0.124 ± 0.047
Benzamil	5	Could not be deduced	0.759 ± 0.406
Doxazosin mesylate	5	0.742 ± 0.533	Could not be deduced

4.7 Thiopermaide - a false positive hit

Thioperamide was one of the hits after the validation assay, having the highest activity of the activators (Figure 4.6). For the EC_{50} experiments, non-transfected HEK293 cells were however used as controls, and while trying to determine the EC_{50} value for VMAT2, it was clearly noticeable that thioperamide also affected substrate uptake in the control as well (Figure 4.12 A). After subtraction of the average of the negative control for each concentration from the corresponding concentration of the hVMAT2 transfected HEK293 cells, the increase in measured fluorescence is quite flat (Figure 4.12 B). A common problem in screening assays based on measurement of fluorescence is that many drugs or compounds have autofluorescent properties that could interfere with the assay. This was not the case for thioperamide however (data not shown), suggesting that the increased fluorescence observed in both transfected and untransfected cells was caused by accumulation of the FFN206 substrate. To figure out whether it was thioperamide itself that affected the cells, or if thioperamide affected the accumulation of FFN206 in the non-transfected HEK293 cells, a concentration dependent assay was set up, where the 96 well plate was split in two, with the same compound concentrations repeated twice. Half of the plate was incubated with FFN206, while the other half was incubated with Opti-MEM™. As expected, there was only detectable fluorescent signal in the wells incubated with FFN206, suggesting that thioperamide

itself has no autofluorescence but rather that it changes accumulation of FFN206 both in transfected and untransfected HEK293 cells (Figure 4.12 C). Finally, we assessed whether the increased FFN206 accumulation upon treatment with thioperamide could be eliminated by preincubation with 200 nM TBZ. As can be seen in Figure 4.12 D, TBZ inhibits accumulation of FFN206 in the VMAT2 transfected HEK293 cells, decreasing the overall substrate uptake in these cells, but the same trend with increasing FFN206 accumulation with increasing thioperamide concentration remain. This indicates that the increase in FFN206 accumulation is unrelated to VMAT2 and occurs through some other mechanism.

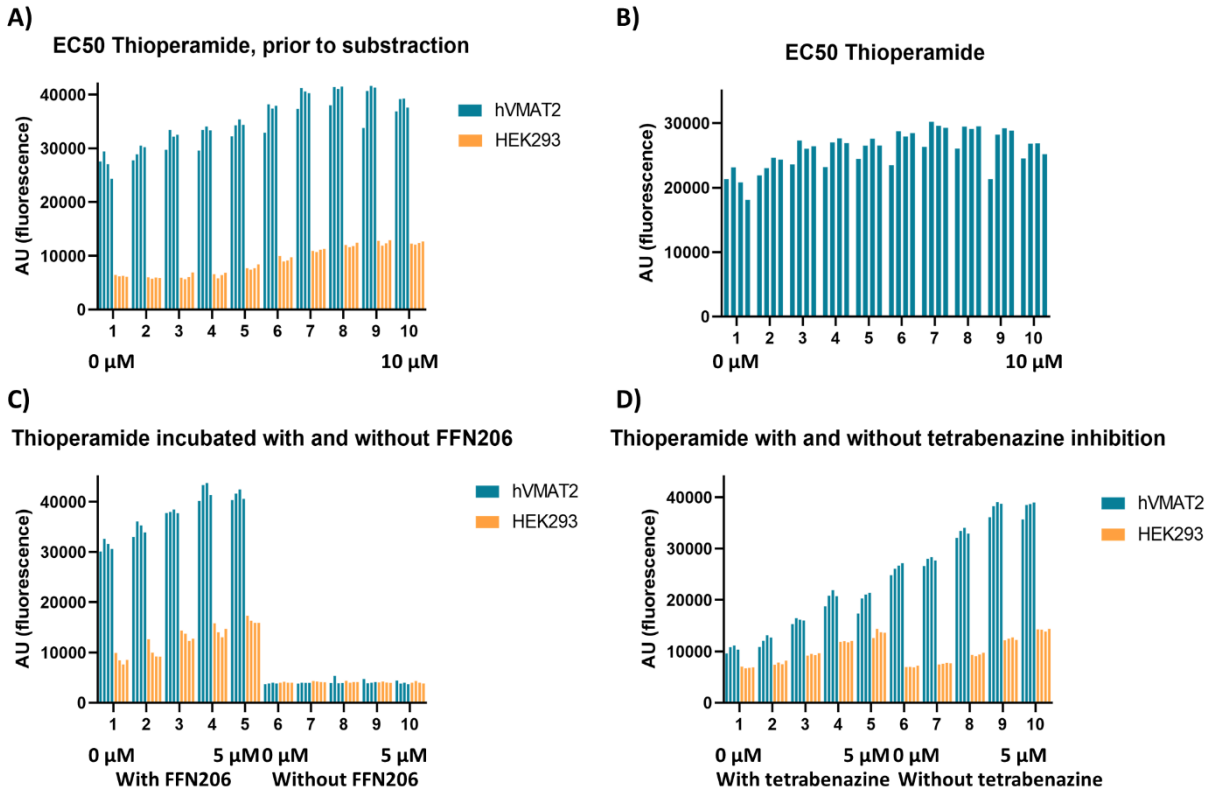

Figure 4.12: ***Thioperamide, a potential false VMAT2 modulator.*** *A: The activity of thioperamide with increasing concentration on hVMAT2 transfected HEK293 cells and the negative control, untransfected HEK293 cells, prior to subtraction of the negative control. B: The activity of thioperamide in hVMAT2 transfected HEK293 cells after subtraction of the negative control, the activity was subtracted for each corresponding concentration. C: Measured fluorescence in cells incubated with (bars marked 1-5) or without (bars marked 6-10) the fluorescent VMAT2 substrate FFN206, demonstrating that it is not thioperamide itself causing the increase in fluorescence due to for instance autofluorescence, but that the drug causes accumulation of FFN206 also in the control cells. D: Assay testing whether the VMAT2 inhibitor tetrabenazine inhibits accumulation of FFN206 in the presence of thioperamide. Bars marked 1-5 was incubated with tetrabenazine together with thioperamide prior to addition of FFN206, bars marked 6-10 was incubated only with thioperamide.*

5 Discussion

Regulation of monoamine neurotransmitter homeostasis is important to maintain neurological functions and dysfunction can lead to neurological and psychiatric diseases such as Parkinson's disease (PD). Accumulating neurotransmitters into synaptic vesicles by VMAT2 is crucial for the subsequent release into the synaptic cleft for further signalling (5). Modulators of VMAT2 have therefore the potential for modifying neurological diseases. Indeed, inhibitors of VMAT 2 are used in the symptomatic treatment of tardive dyskinesia and chorea associated with Huntington's disease (3), while activators have a potential for symptomatic treatment of PD in combination with L-DOPA (5). PD is today often treated with levodopa, a precursor for DA, temporarily replacing the loss of midbrain DA, but this treatment does not prevent loss of dopaminergic neurons (36). Levodopa treatment causes a burst of DA synthesis in the cells, but an increase in DA levels will have a low effect if DA is not transported into synaptic vesicles for further signalling by VMAT2 (5). A study performed by Pifl et al., comparing DA storage vesicles from autopsied brains from control and PD patients, discovered a defect in DA uptake by VMAT2, appearing to be specific for PD patients (39). It seems that the defect in DA storage is at VMAT2 itself (39), and activators or stabilizers of VMAT2 that can increase or maintain its activity, have therefore a potential use in future treatment of PD. Developing a high throughput functional screening assay for VMAT2 enables a quick and easy method to screen for new modulators affecting VMAT2 function.

5.1 High-throughput screening assay

There are several approaches for high-throughput screening of protein targets. These include biophysical screening approaches, such as for instance by differential scanning fluorimetry (DSF), *in silico* screening approaches, where all screenings are performed virtually by docking and MD simulations, and cell-based screening approaches. All these methodologies have strengths and weaknesses. Biophysical screenings are easier to perform, can have high throughput, and will identify compounds that directly bind to the target protein. Biophysical screening approaches do however require large amounts of purified protein, which is expensive and difficult for membrane proteins. In silico screening is on the other hand fairly cheap, but it requires a high-resolution protein structure, and all results require follow up by thorough experimental validation. Cellular

screening enables for identifying compounds with a direct effect in cells, either by increased protein levels or by altering protein function without suited robotics, cell-based screening can be laboursome.

For VMAT2 there are no high resolution protein structures available that are good enough to do in silico screening (1), and the protein is difficult and expensive to express and purify (63). We therefore set out to establish a cell-based screening approach for VMAT2 using the fluorescent VMAT substrate FFN206 (91), and screened the same compound library as was previously done by DSF (63), to directly compare results, and to supplement with additional hits, as different methods typically give different hits.

We successfully set up an assay screening 80 different compounds at once in one 96 well plate with hVMAT2 transfected HEK293 cells using the VMAT2 substrate FFN206. The screening assay with FFN206 is robust and easy to perform and can be used for screening both VMAT1 and VMAT2. HEK293 cells works fine, but for future screening campaigns using this method a stably transfected cell line that constitutively express VMAT2 should be considered. Stably transfected cells would increase the throughput and reduce costs related to large scale transfections. Pipetting robots which can handle plates at 384 wells would also lead to higher throughput for the assay, though this is not available at our department. Stable transfected cells could also increase the reproducibility in the experiments, as there would be less variation between cells used in each assay. Transiently transfected cells however have the advantage of easily being able to test VMAT2 variants if desired. Such studies could be performed to validate binding of hit compounds. Other cell lines might also be suitable for the assay, for example neuronal cells naturally expressing VMAT2, although neuronal cell models typically will grow at a slower rate and are less robust.

The developed assay is functionable, detecting inhibitors of VMAT2 at low concentrations, and can be used both for the initial screening and to determine IC_{50} values for each hit compound. When comparing the hits found in this functional screening with the screening using DSF performed by Støve et al (63), many of the hits were the same. Five out of seven of the hits from DSF screening that had an IC_{50} value below 2 µM were also among the hits in this cellular screening assay, but in addition we discovered 3 additional potent inhibitors with an IC_{50} below 2 µM that were not found

by DSF. In addition to the two known VMAT2 inhibitors that were excluded from further validation studies, only one of thirteen compounds fulfilling our hit criteria after the concentration dependent validation assay were found among the DSF results. These methods can therefore complement each other when screening for modulators of the same protein.

One weakness of the present fluorescence-based HTS assay is auto-fluorescent compounds in the library. If a compound is auto-fluorescent it might give false activating hits or inhibiting compounds might not be identified, as their activity would be falsely high. Due to this weakness the hits should be further validated using a different method, independent of fluorescence. Another weakness with this screening approach is that the cell media, compounds, and PBS are manually removed by pipetting, which may result in irregular washing. By screening all compounds at two concentrations however and comparing the results for the same compounds in two individual plates, the likeliness of these false hits is reduced. The manual pipetting can also scrape of some cells from the wells and some cells might get washed away during the washing steps, potentially leading to reduced measured activity. When setting up the measurement method, choosing to measure several spots in one well is likely to give a more accurate average of the activity as the activity is then not dependent on one small area being representative for the whole well. In our experiments, all wells in the 96 well plate were measured 16 times at different places in the well and the signal from these measurements was averaged.

5.2 Determination of EC_{50} and IC_{50} values for VMAT2

When analysing results from the screening, the activity of the control (untransfected HEK293 cells) was subtracted from the measured activity of the transfected cells. A difference in confluency between the untransfected and the transfected cells has therefore the possibility to give false high or low activity of the transfected cells when calculating IC_{50} and EC_{50} values, and one should therefore aim to have the same confluency in both the transfected and untransfected cells.

For the IC_{50} and EC_{50} experiments some compounds had varying range of values between the individual repetitions, making it hard to deduce an IC_{50} and EC_{50} value, which is the reason for the difference in number of repetitions for compounds. Some of these variations were due to a poor

control. The control could have several unsystematically high or low values, complicating the calculation. Due to the auto fluorescence in some compounds which also increases the activity of the control cells at the highest concentration, the average activity of the control was calculated for each concentration, prior to subtraction from the VMAT transfected cells for the equivalent concentration.

The STD for the compounds is varying (Table 4.3), gatifloxacin which has a flat curve with bad fit (Figure 4.9 B), has an STD 0.427 for VMAT2, which is nearly the same as the calculated EC_{50} value of 0.450. (+)-Isoproterenol (+)-bitartrate salt had a low STD compared to the EC_{50} value for VMAT2, but the EC_{50} value is unreliable due to the flat curve and poor fitting (Figure 4.9A).

5.3 Inhibitor displacement assay

In the inhibitor displacement assay, cell lysates were preincubated with a high concentration of hit compounds (50 µM) before 2 nM [^{3}H] HTBZ and 15 nM [^{3}H] salmeterol were added to the mixture. This large difference is in correspondence with what has been seen previously for reserpine, which despite being a highly potent inhibitor of VMAT2 needed concentrations up to 400-fold the concentration of [^{3}H] HTBZ to achieve a 50% reduction in [^{3}H] HTBZ (19). In our inhibitor displacement assay only one concentration of hit-compounds was assayed, giving little information about how efficiently the hit compounds were competing with [^{3}H] HTBZ. To acquire more information, all compounds should be tested in a concentration dependent matter to determine IC50 values of inhibitor displacement. Due to time limitations, and lack of [^{3}H] HTBZ reagents these assays could not be performed in the current work. Also, this assay was performed twice and should ideally have been repeated a third time.

For the compounds competing with [^{3}H] HTBZ and [^{3}H] salmeterol in our assays, the results indicate either that they bind at the same location in VMAT2 or that they induce a conformational change in the transporter that hides the TBZ and salmeterol binding site. Both TBZ and salmeterol have been shown to bind in the central cavity of the transporter (63).The compounds that did not show any competition with [^{3}H] HTBZ and [^{3}H] salmeterol, might still directly interact with

VMAT2 either with lower affinity, or they might bind at a differing binding site that does not affect [^{3}H] HTBZ and [^{3}H] salmeterol binding.

5.4 VMAT2 specificity

While obtaining IC50 values for VMAT1, benzamil did not flatten out, making the calculation of a value inaccurate, and sometimes not possible (Figure 9.4). Increasing the concentration did not help as compound is auto fluorescent, the activity starts to increase with increasing concentrations, and do not flatten out the curve either. Even though there are no determined IC_{50} value for benzamil, it might still be VMAT2 specific as a concentration of 270 µM was not enough to determine a value. We could not determine the EC_{50} value for VMAT1 for (+)-isoproterenol (+)-bitartrate salt due to poor fitting of the curve (Figure 4.11A and 9.4) and cannot be compared to EC_{50} value for VMAT2 (Table 4.5), which was also unreliable. Gatifloxacin's EC_{50} value for VMAT1 is lower than that for VMAT2 (Table 4.5), indicating that gatifloxacin might not be VMAT2 specific, but due to the unreliable EC_{50} value for VMAT2, we cannot conclude with that.

5.5 A potential false positive hit

Thioperamide seems to affect the HEK293 cells themselves and not only VMAT2, as the activity in the control followed the measured activity of the transfected cells, without seeing the same pattern when measuring fluorescence of the compound solutions used in the assay itself. Subtracting the average from the control, gave a flat curve with little sign of activation (Figure 4.12 B). We tested it if it was the compound itself that gave the activity in the control, or if the cells accumulate FFN206, which they did. Next, we tested if accumulation of FFN206 was inhibited by TBZ, which it was, but not completely. Thioperamide might affect VMAT2, but one cannot say that for sure as they also affect the HEK293 cells ability to accumulate FFN206. This compound illustrates the importance of having the right control, as another control might not have picked up thioperamides effect on the HEK293 cells.

5.6 Evaluation of hit compounds

SwissADME has been used to determine the ability of hit compounds to penetrate the blood brain barrier (BBB) using the Brain Or IntestinaL EstimateD permeation (BOILED-Egg) method (92, 93), and the possibility of them being false hits, by checking for pan assay interference compounds (PAINS) alerts (92). To affect VMAT2 in the CNS, compound should be able to penetrate BBB. If a drug is not able to penetrate BBB, it is possible to optimize properties to aim for penetration (93), but requiring more testing and further derivatization. In general, all compounds included in the Prestwick Chemical Library are, or have been, FDA approved drugs that are suitable for drug repurposing or drug derivatization campaigns (94). Their druglikeness and bioavailability score has thus already been assessed, and will not be further discussed.

5.6.1 (+)-Isoproterenol (+)-bitartrate salt

(+)-Isoproterenol (+)-bitrartrate salt is a nonselective β-adrenergic receptor agonist, first approved for treatment of bronchial asthma, it was also used for chronic obstructive pulmonary disease (COPD). It has also cardiovascular effects, such as vasodilation, inotropy and chronotropy, and it is used after heart transplant to control bradyarrhythmia. Its usage towards bronchial asthma and COPD declined when selective β2-agonists were discovered (76). It has been indicated that β-adrenoceptor agonists increase BBB's permeability, but the studies performed are inconclusive (95). Olesen et al performed a study on isoproterenol ability to penetrate BBB in humans, and the mean extraction they got after a single passage through the brain circulation was 3.8%, while for propranolol in comparison it was 63% (96). According to SwissADME, (+)-isoproterenol (+)-bitartrate salt is not BBB permeable, and it has one PAINS alert, the catechol group of the structure (92). Despite the PAINS alert for the catechol group however, it is not unlikely that isoproterenol binds to VMAT2 as it is an analogue of epinephrine (Figure 1.6 and Figure 4.7), a VMAT2 substrate. It is also interesting as several other β2-adrenergic agonist (salmeterol, formoterol) were previously shown as tight binders and potent inhibitors of VMAT2 (63).

5.6.2 Gatifloxacin

Gatifloxacin is an extended-spectrum antibacterial agent, active against both gram negative and positive bacteria. It is an 8-methoxy fluoroquinolone with a 3-methylpipazinyl group at C7 (Figure 4.7). Orally applied gatifloxacin distributes to tissue, but also to CNS (87). According to SwissADME it is not BBB permeable, and it has no PAINS alert. Even though SwissADME states it is not BBB permeable (92), Perry et al. state that it distributes to CNS, as they have measured the serum concentration in cerebrospinal fluid and found gatifloxacin (87). Another study by Li et al suggests that Na^+/Ca^{2+} exchange mechanism and extracellular Ca^{2+} is involved in the transport of gatifloxacin across rat brain micro vessel endothelial cells (97). A nanocarrier has also been developed for the passage of gatifloxacin through BBB for treatment of CNS tuberculosis (98), also making it a potential hit compound for further development into a specific VMAT2 activator.

5.6.3 Doxazosin mesylate

The selective alfa-1a-adrenoceptor antagonist doxazosin mesylate (90) reduces peripheral vascular resistance and vasodilation by antagonising the activity of noradrenaline at the postjunctional adrenergic receptors (99). Noradrenaline is a VMAT2 substrate (13). Doxazosin mesylate is used for a variety of diseases as a complementary drug, for instance hypertension and benign prostatic hyperplasia. SwissADME states that it has no PAINS alerts and is not BBB permeable (92), but common side effects are CNS related (99), indicating that doxazosin mesylate affects the CNS. According to Pool et al. it is documented that alfa-1a-adrenergic antagonist can cross the BBB (90), and there are also more specific indications that doxazosin reaches the CNS (100). The IC_{50} value of doxazosin mesylate could not be determined due to variations in both the VMAT2-transfected and the untransfected HEK293 cells, but it does reduce binding of [^{3}H] HTBZ and [^{3}H] salmeterol with approximately 70% (Figure 4.10), indicating direct interaction with VMAT2. The result should be treated with caution, but doxazosin mesylate seems as a hit compound for further development.

5.6.4 Benzamil (hydrochloride)

Benzamil hydrochloride interacts with the renin angiotensin aldosteron system (RAAS), acting on epithelial sodium channel (89). Benzamil also inhibits the Na^{2+}/Ca^{2+} exchanger, and regulates transient elevation of Ca^{2+} in neurons through inhibition of other targets, such as small conductance Ca^{2+} activated K^{+} channels (101). Benzamil has no PAINS alert and does not penetrate the BBB (92), and the lack of BBB permeability makes it likely unable to affect VMAT2 directly in CNS. Benzamil does compete with [^{3}H] HTBZ and [^{3}H] salmeterol with approximately 50% (Figure 4.10), indicating binding to VMAT2 in a way that can compete with [^{3}H] HTBZ and [^{3}H] salmeterol. It had a IC_{50} value of 0.759 ± 0.406 for VMAT2, the IC_{50} value for VMAT1 could not be determined due to the curve (Appendix Figure 9.4), however it might still show some VMAT2 specificity as the value would be markedly higher than for VMAT2. Further derivatization of the compound is necessary for benzamil to penetrate the BBB and affect VMAT2 in the CNS.

5.6.5 Prenylamine lactate

Prenylamine lactate, a calcium channel blocker is an antialgal drug withdrawn from the marked in 1988, due to proarrhythmia associated with prolonged QT interval (88). Prenylamine lactate inhibits reuptake of noradrenaline into storage vesicles in sympathetic tissue and its release, causing depleting of noradrenaline from endogenous storage in adrenergic nerves and ganglia. It uncouples the ATPase, partly inhibiting the transmembrane proton electrochemical gradient created by the H^{+}-ATPase (102). It also increases the concentration of DA and noradrenaline in the synaptic cleft by preventing the reuptake by storage granules, possibly suppressing seizures (103). In our assays prenylamine was a potent inhibitor of both VMAT1 and VMAT2 with an IC_{50} of 0.417 ± 0.201 and 0.124 ± 0.047, respectively. Due to the prenylamine's inhibiting effect on the H^{+}-ATPase and the disruption of the vesicular proton gradient (102), our inhibitor displacement assay showing direct competition of binding with [^{3}H] HTBZ and [^{3}H] salmeterol (Figure 4.10) also suggests that it binds directly to VMAT2 and thus also might affect VMAT2 function. According to SwissADME, it does not penetrate the BBB and has no PAINS alert (92), which means that further experimentation is needed to reach VMAT2 in the CNS.

5.6.6 Trimebutine

Trimebutine is used for symptomatic treatment of irritable bowel syndrome (IBS), altering bowel habits and reliving abdominal pain (79). Release of gastrointestinal peptides and modulation of others peptides is one of the ways trimebutine mediate a response, it also has an agonist effect on the peripheral opioid receptors kappa, delta and mu (104). According to SwissADME, the PAINS score for trimebutine is zero and it is likely to penetrate BBB (92, 93) but according to Kountouras et al. there is no evidence indicating CNS affection following trimebutine treatment (104). Trimebutine has low IC_{50} values for VMAT1 and VMAT2, i.e 0.411 ± 0.232 µM and 0.205 ± 0.155 µM respectively. Trimebutine does not compete with [^{3}H] HTBZ and [^{3}H] salmeterol (Figure 4.10), it might still have a direct interaction with VMAT2, but have lower affinity or bind at a different site of the transporter. Considering the SwissADME prediction of its BBB penetration, trimebutine has a potential as inhibitor VMAT2.

6 Conclusion

One of the main aims for this thesis was to establish a cellular screening assay for VMAT2 based on the VMAT2 substrate and VMAT2 transfected HEK293 cells. The second aim for this thesis was to identify new modulators of VMAT2 activity, for potential repurposing of already approved drugs. The assay gave 55 initial hits from screening of the Prestwick chemical library®, which was further reduced to seven hits after a concentration dependent validation assay. Although potential activators were discovered, the screening did not result in the identification of any modulators we can conclude with certainty that activate VMAT2, but we found several inhibitors inhibiting VMAT2 with an IC50 that was lower than 1 μM and which can be a great starting point for further drug derivatization.

7 Future perspectives

The developed screening assay could be further improved by stable transfecting cells which continually expresses VMAT (either VMAT2 or VMAT1), giving an even amount of VMAT between each experiment, and it would increase the throughput by saving the time used on transfecting the cells between each assay. Expanding the screening set up to 384 well plates with robotics, instead of 96 well plates would also drastically increase the throughput of the assay.

To further investigate how the compounds modulate VMAT2 activity and if they affect VMAT2 directly or indirectly, direct binding experiments should be performed, for instance by acquiring radiolabelled hit compounds in assays with purified protein, or biophysical approaches such as surface plasmon resonance or bio-layer interferometry. Another assay to measure the effect on substrate uptake by VMAT2 in a less complex system would be to measure uptake of FFN206 in purified vesicles or using purified protein reconstituted in liposomes.

Finally, once direct binding to VMATs have been shown, to learn more about which residues are important in for the binding between the compound and the protein, one could do molecular docking of compounds to a VMAT2 homology model in combination with site-directed mutagenesis to study how different residues contribute to drug binding. Studying whether the compounds are competitive or non-competitive modulators of VMAT2, would also give more information on how they bind.

To further expand the screening campaign, all hit compounds could be clustered together with all previously known VMAT2 inhibitors and all compounds of larger compound libraries to identify clusters of similar compounds that might also affect VMAT2 function. This is a powerful technique for identification of new clusters of other similar compounds in larger compound libraries (such as for instance our in-house Myriad screening library with 10 000 compounds). This type of clustering and analysis can be performed using the Schrodinger Maestro and Canvas software in a similar manner as was performed in this work (Figure 4.4).

8 References

1. Yaffe D, Forrest LR, Schuldiner S. The ins and outs of vesicular monoamine transporters. Journal of General Physiology. 2018;150(5):671-82.
2. Chaudhry FA, Edwards RH, Fonnum F. Vesicular Neurotransmitter Transporters as Targets for Endogenous and Exogenous Toxic Substances. Annual Review of Pharmacology and Toxicology. 2008;48(1):277-301.
3. Koch J, Shi W-X, Dashtipour K. VMAT2 inhibitors for the treatment of hyperkinetic movement disorders. Pharmacology & Therapeutics. 2020;212:107580.
4. Wimalasena K. Vesicular monoamine transporters: Structure-function, pharmacology, and medicinal chemistry. Medicinal Research Reviews. 2011;31(4):483-519.
5. Bernstein AI, Stout KA, Miller GW. The vesicular monoamine transporter 2: An underexplored pharmacological target. Neurochemistry International. 2014;73:89-97.
6. Pizzagalli MD, Bensimon A, Superti-Furga G. A guide to plasma membrane solute carrier proteins. The FEBS Journal. 2021;288(9):2784-835.
7. Lohoff FW, Carr GV, Brookshire B, Ferraro TN, Lucki I. Deletion of the vesicular monoamine transporter 1 (vmat1/slc18a1) gene affects dopamine signaling. Brain Research. 2019;1712:151-7.
8. Sievers F, Wilm A, Dineen D, Gibson TJ, Karplus K, Li W, et al. Fast, scalable generation of high-quality protein multiple sequence alignments using Clustal Omega. Molecular Systems Biology. 2011;7(1):539.
9. Jumper J, Evans R, Pritzel A, Green T, Figurnov M, Ronneberger O, et al. Highly accurate protein structure prediction with AlphaFold. Nature. 2021;596(7873):583-9.
10. Varadi M, Anyango S, Deshpande M, Nair S, Natassia C, Yordanova G, et al. AlphaFold Protein Structure Database: massively expanding the structural coverage of protein-sequence space with high-accuracy models. Nucleic Acids Research. 2022;50(D1):D439-D44.
11. Perland E, Bagchi S, Klaesson A, Fredriksson R. Characteristics of 29 novel atypical solute carriers of major facilitator superfamily type: evolutionary conservation, predicted structure and neuronal co-expression. Open Biology. 2017;7(9):170142.
12. Lawal HO, Krantz DE. SLC18: Vesicular neurotransmitter transporters for monoamines and acetylcholine. Molecular Aspects of Medicine. 2013;34(2-3):360-72.
13. Moriyama Y, Hatano R, Moriyama S, Uehara S. Vesicular polyamine transporter as a novel player in amine-mediated chemical transmission. Biochimica et Biophysica Acta (BBA) - Biomembranes. 2020;1862(12):183208.
14. Coleman JA, Yang D, Zhao Z, Wen P-C, Yoshioka C, Tajkhorshid E, et al. Serotonin transporter–ibogaine complexes illuminate mechanisms of inhibition and transport. Nature. 2019;569(7754):141-5.
15. Coleman JA, Green EM, Gouaux E. X-ray structures and mechanism of the human serotonin transporter. Nature. 2016;532(7599):334-9.
16. Wang KH, Penmatsa A, Gouaux E. Neurotransmitter and psychostimulant recognition by the dopamine transporter. Nature. 2015;521(7552):322-7.
17. Penmatsa A, Wang KH, Gouaux E. X-ray structure of dopamine transporter elucidates antidepressant mechanism. Nature. 2013;503(7474):85-90.
18. Yaffe D, Radestock S, Shuster Y, Forrest LR, Schuldiner S. Identification of molecular hinge points mediating alternating access in the vesicular monoamine transporter VMAT2. Proceedings of the National Academy of Sciences. 2013;110(15):E1332-E41.

19. Yaffe D, Vergara-Jaque A, Forrest LR, Schuldiner S. Emulating proton-induced conformational changes in the vesicular monoamine transporter VMAT2 by mutagenesis. Proceedings of the National Academy of Sciences. 2016;113(47):E7390-E8.
20. Anne C, Gasnier B. Vesicular Neurotransmitter Transporters. Elsevier; 2014. p. 149-74.
21. Drew D, North RA, Nagarathinam K, Tanabe M. Structures and General Transport Mechanisms by the Major Facilitator Superfamily (MFS). Chemical Reviews. 2021;121(9):5289-335.
22. Huang H, Li Y, Liang J, Finkelman FD. Molecular Regulation of Histamine Synthesis. Front Immunol. 2018;9:1392-.
23. Hussain LS, Reddy V, Maani CV. Physiology, Noradrenergic Synapse. StatPearls. Treasure Island (FL): StatPearls Publishing
Copyright © 2022, StatPearls Publishing LLC.; 2022.
24. Fernstrom JD, Fernstrom MH. Tyrosine, Phenylalanine, and Catecholamine Synthesis and Function in the Brain. The Journal of Nutrition. 2007;137(6):1539S-47S.
25. Klein MO, Battagello DS, Cardoso AR, Hauser DN, Bittencourt JC, Correa RG. Dopamine: Functions, Signaling, and Association with Neurological Diseases. Cellular and Molecular Neurobiology. 2019;39(1):31-59.
26. German CL, Baladi MG, McFadden LM, Hanson GR, Fleckenstein AE. Regulation of the Dopamine and Vesicular Monoamine Transporters: Pharmacological Targets and Implications for Disease. Pharmacological Reviews. 2015;67(4):1005-24.
27. Rubí B, Maechler P. Minireview: New Roles for Peripheral Dopamine on Metabolic Control and Tumor Growth: Let's Seek the Balance. Endocrinology. 2010;151(12):5570-81.
28. Puttonen HAJ, Semenova S, Sundvik M, Panula P. Storage of neural histamine and histaminergic neurotransmission is VMAT2 dependent in the zebrafish. Scientific Reports. 2017;7(1).
29. Tillinger A, Sollas A, Serova LI, Kvetnansky R, Sabban EL. Vesicular Monoamine Transporters (VMATs) in Adrenal Chromaffin Cells: Stress-Triggered Induction of VMAT2 and Expression in Epinephrine Synthesizing Cells. Cellular and Molecular Neurobiology. 2010;30(8):1459-65.
30. Berger M, Gray JA, Roth BL. The Expanded Biology of Serotonin. Annual Review of Medicine. 2009;60(1):355-66.
31. Francescangeli J, Karamchandani K, Powell M, Bonavia A. The Serotonin Syndrome: From Molecular Mechanisms to Clinical Practice. International Journal of Molecular Sciences. 2019;20(9):2288.
32. Daubert EA, Heffron DS, Mandell JW, Condron BG. Serotonergic dystrophy induced by excess serotonin. Molecular and Cellular Neuroscience. 2010;44(3):297-306.
33. Nuutinen S, Panula P. Histamine in Neurotransmission and Brain Diseases. Springer US; 2010. p. 95-107.
34. Baronio D, Chen YC, Decker AR, Enckell L, Fernández-López B, Semenova S, et al. Vesicular monoamine transporter 2 (SLC18A2) regulates monoamine turnover and brain development in zebrafish. Acta Physiologica. 2022;234(1).
35. Armstrong MJ, Okun MS. Diagnosis and Treatment of Parkinson Disease. JAMA. 2020;323(6):548.
36. Chinta SJ, Andersen JK. Dopaminergic neurons. The International Journal of Biochemistry & Cell Biology. 2005;37(5):942-6.
37. Masato A, Plotegher N, Boassa D, Bubacco L. Impaired dopamine metabolism in Parkinson's disease pathogenesis. Molecular Neurodegeneration. 2019;14(1).

38. Hare DJ, Double KL. Iron and dopamine: a toxic couple. Brain. 2016;139(4):1026-35.
39. Pifl C, Rajput A, Reither H, Blesa J, Cavada C, Obeso JA, et al. Is Parkinson's Disease a Vesicular Dopamine Storage Disorder? Evidence from a Study in Isolated Synaptic Vesicles of Human and Nonhuman Primate Striatum. Journal of Neuroscience. 2014;34(24):8210-8.
40. Lerner RP, Francardo V, Fujita K, Bimpisidis Z, Jourdain VA, Tang CC, et al. Levodopa-induced abnormal involuntary movements correlate with altered permeability of the blood-brain-barrier in the basal ganglia. Scientific Reports. 2017;7(1).
41. Brooks DJ. Dopamine agonists: their role in the treatment of Parkinson's disease. Journal of Neurology, Neurosurgery & Psychiatry. 2000;68(6):685-9.
42. Brocks DR. Anticholinergic drugs used in Parkinson's disease: An overlooked class of drugs from a pharmacokinetic perspective. J Pharm Pharm Sci. 1999;2(2):39-46.
43. Antonini A, Barone P, Ceravolo R, Fabbrini G, Tinazzi M, Abbruzzese G. Role of Pramipexole in the Management of Parkinson’s Disease. CNS Drugs. 2010;24(10):829-41.
44. Rilstone JJ, Alkhater RA, Minassian BA. Brain Dopamine–Serotonin Vesicular Transport Disease and Its Treatment. New England Journal of Medicine. 2013;368(6):543-50.
45. Stahl SM. Mechanism of action of vesicular monoamine transporter 2 (VMAT2) inhibitors in tardive dyskinesia: reducing dopamine leads to less “go” and more “stop” from the motor striatum for robust therapeutic effects. CNS Spectrums. 2018;23(1):1-6.
46. Limandri BJ. Tardive Dyskinesia: New Treatments Available. Journal of Psychosocial Nursing & Mental Health Services. 2019;57(5):11-4.
47. Tarakad A, Jimenez-Shahed J. VMAT2 Inhibitors in Neuropsychiatric Disorders. CNS Drugs. 2018;32(12):1131-44.
48. Solmi M, Pigato G, Kane JM, Correll C. Treatment of tardive dyskinesia with VMAT-2 inhibitors: a systematic review and meta-analysis of randomized controlled trials. Drug Design, Development and Therapy. 2018;Volume 12:1215-38.
49. Eiden LE, Weihe E. VMAT2: a dynamic regulator of brain monoaminergic neuronal function interacting with drugs of abuse. Annals of the New York Academy of Sciences. 2011;1216(1):86-98.
50. Schneider F, Stamler D, Bradbury M, Loupe PS, Hellriegel E, Cox DS, et al. Pharmacokinetics of Deutetrabenazine and Tetrabenazine: Dose Proportionality and Food Effect. Clinical Pharmacology in Drug Development. 2021;10(6):647-59.
51. Dean J, Keshavan M. The neurobiology of depression: An integrated view. Asian Journal of Psychiatry. 2017;27:101-11.
52. Nickell JR, Siripurapu KB, Vartak A, Crooks PA, Dwoskin LP. The Vesicular Monoamine Transporter-2. Elsevier; 2014. p. 71-106.
53. Lohr KM, Stout KA, Dunn AR, Wang M, Salahpour A, Guillot TS, et al. Increased Vesicular Monoamine Transporter 2 (VMAT2; Slc18a2) Protects against Methamphetamine Toxicity. ACS Chemical Neuroscience. 2015;6(5):790-9.
54. Lee N-R, Zheng G, Leggas M, Janganati V, Nickell JR, Crooks PA, et al. GZ-11608, a Vesicular Monoamine Transporter-2 Inhibitor, Decreases the Neurochemical and Behavioral Effects of Methamphetamine. Journal of Pharmacology and Experimental Therapeutics. 2019;371(2):526-43.
55. Shih JC, Ridd MJ, Chen K, Meehan WP, Kung M-P, Seif I, et al. Ketanserin and tetrabenazine abolish aggression in mice lacking monoamine oxidase A. Brain Research. 1999;835(2):104-12.

56. Meyer AC, Neugebauer NM, Zheng G, Crooks PA, Dwoskin LP, Bardo MT. Effects of VMAT2 inhibitors lobeline and GZ-793A on methamphetamine-induced changes in dopamine release, metabolism and synthesis in vivo. Journal of Neurochemistry. 2013;127(2):187-98.
57. Hu G, Henke A, Karpowicz RJ, Sonders MS, Farrimond F, Edwards R, et al. New Fluorescent Substrate Enables Quantitative and High-Throughput Examination of Vesicular Monoamine Transporter 2 (VMAT2). ACS Chemical Biology. 2013;8(9):1947-54.
58. Wang W, Du G, Lin S, Liu J, Yang H, Yu D, et al. (+)-9-Trifluoroethoxy-α-Dihydrotetrabenazine as a Highly Potent Vesicular Monoamine Transporter 2 Inhibitor for Tardive Dyskinesia. Front Pharmacol. 2021;12:770377-.
59. Lohr KM, Bernstein AI, Stout KA, Dunn AR, Lazo CR, Alter SP, et al. Increased vesicular monoamine transporter enhances dopamine release and opposes Parkinson disease-related neurodegeneration in vivo. Proceedings of the National Academy of Sciences. 2014;111(27):9977-82.
60. Pulix M, Lukashchuk V, Smith DC, Dickson AJ. Molecular characterization of HEK293 cells as emerging versatile cell factories. Current Opinion in Biotechnology. 2021;71:18-24.
61. Lynch J, Chung J, Huang Z, Pierce V, Saunders NS, Niu L. Enhancing transient protein expression in HEK-293 cells by briefly exposing the culture to DMSO. Journal of Neuroscience Methods. 2021;350:109058.
62. Thomas P, Smart TG. HEK293 cell line: A vehicle for the expression of recombinant proteins. Journal of Pharmacological and Toxicological Methods. 2005;51(3):187-200.
63. Støve SI, Skjevik ÅA, Teigen K, Martinez A. β2-adrenergic agonists and the atypical antipsychotic ziprasidone inhibit VMAT2. Communications Biology. *in review*.
64. Gao K, Oerlemans R, Groves MR. Theory and applications of differential scanning fluorimetry in early-stage drug discovery. Biophysical Reviews. 2020;12(1):85-104.
65. Seeger TF, Seymour PA, Schmidt AW, Zorn SH, Schulz DW, Lebel LA, et al. Ziprasidone (CP-88,059): a new antipsychotic with combined dopamine and serotonin receptor antagonist activity. J Pharmacol Exp Ther. 1995;275(1):101-13.
66. Li Z, Lu M, Luo Z, Chen H, Li J, Zhang C, et al. Roles of dopamine receptors and their antagonist thioridazine in hepatoma metastasis. OncoTargets and Therapy. 2015:1543.
67. Peniche AG, Osorio EY, Melby PC, Travi BL. Efficacy of histamine H1 receptor antagonists azelastine and fexofenadine against cutaneous Leishmania major infection. PLOS Neglected Tropical Diseases. 2020;14(8):e0008482.
68. Stoschitzky K, Stoschitzky G, Lercher P, Brussee H, Lamprecht G, Lindner W. Propafenone shows class Ic and class II antiarrhythmic effects. Europace. 2016;18(4):568-71.
69. Mellstrand T. Loperamide--an opiate receptor agonist with gastrointestinal motility effects. Scand J Gastroenterol Suppl. 1987;130:65-6.
70. Stubberud A, Flaaen NM, McCrory DC, Pedersen SA, Linde M. Flunarizine as prophylaxis for episodic migraine: a systematic review with meta-analysis. Pain. 2019;160(4):762-72.
71. Williams K. Ifenprodil, a novel NMDA receptor antagonist: site and mechanism of action. Curr Drug Targets. 2001;2(3):285-98.
72. Cho YS, Yen C-N, Shim JS, Kang DH, Kang SW, Liu JO, et al. Antidepressant indatraline induces autophagy and inhibits restenosis via suppression of mTOR/S6 kinase signaling pathway. Scientific Reports. 2016;6(1):34655.
73. Meyer JM, Wenzel CL, Kradjan WA. Salmeterol: A Novel, Long-Acting Beta2-Agonist. Annals of Pharmacotherapy. 1993;27(12):1478-87.
74. Carter BL. Labetalol. Drug Intell Clin Pharm. 1983;17(10):704-12.

75. Ruffolo JRR, Feuerstein GZ. Cardiovascular Drugs and Therapy. 1997;11(1+):247-56.
76. D'Ambrosi J, Amin N. Hyperinflation of Isoproterenol. Journal of Pharmacy Practice. 2018;31(4):390-4.
77. MacCarthy EP, Bloomfield SS. Labetalol: a review of its pharmacology, pharmacokinetics, clinical uses and adverse effects. Pharmacotherapy. 1983;3(4):193-219.
78. Baker JG. The selectivity of β -adrenoceptor antagonists at the human β 1, β 2 and β 3 adrenoceptors. British Journal of Pharmacology. 2005;144(3):317-22.
79. Lee H-T, Kim BJ. Trimebutine as a modulator of gastrointestinal motility. Archives of Pharmacal Research. 2011;34(6):861-4.
80. Daniluk J, Malecka-Wojciesko E, Skrzydlo-Radomanska B, Rydzewska G. The Efficacy of Mebeverine in the Treatment of Irritable Bowel Syndrome—A Systematic Review. Journal of Clinical Medicine. 2022;11(4):1044.
81. Chen X, Geiger JD. Janus sword actions of chloroquine and hydroxychloroquine against COVID-19. Cellular Signalling. 2020;73:109706.
82. Jung DW, Brierley GP. Energy-Dependent contraction of swollen heart mitochondria—Activation by butacaine. Archives of Biochemistry and Biophysics. 1979;193(1):76-87.
83. El-Boghdadly K, Pawa A, Chin KJ. Local anesthetic systemic toxicity: current perspectives. Local and Regional Anesthesia. 2018;Volume 11:35-44.
84. Garcia-Ladona FJ, Cox BF. BP 897, a Selective Dopamine D3 Receptor Ligand with Therapeutic Potential for the Treatment of Cocaine-Addiction. CNS Drug Reviews. 2006;9(2):141-58.
85. Refai O, Blakely RD. Blockade and reversal of swimming-induced paralysis in C. elegans by the antipsychotic and D2-type dopamine receptor antagonist azaperone. Neurochemistry International. 2019;123:59-68.
86. Van Boven M, Daenens P. Analysis and Identification of Azaperone and Its Metabolites in Humans. Journal of Analytical Toxicology. 1992;16(1):33-5.
87. Perry CM, Barman Balfour JA, Lamb HM. Gatifloxacin. Drugs. 1999;58(4):683-96.
88. Shah RR, Stonier PD. Withdrawal of prenylamine: perspectives on pharmacological, clinical and regulatory outcomes following the first QT-related casualty. Therapeutic Advances in Drug Safety. 2018;9(8):475-93.
89. Abrams JM, Osborn JW. A ROLE FOR BENZAMIL-SENSITIVE PROTEINS OF THE CENTRAL NERVOUS SYSTEM IN THE PATHOGENESIS OF SALT-DEPENDENT HYPERTENSION. Clinical and Experimental Pharmacology and Physiology. 2008;35(5-6):687-94.
90. Pool JL, Kirby RS. Clinical significance of α1-adrenoceptor selectivity in the management of benign prostatic hyperplasia. International Urology and Nephrology. 2001;33(3):407-12.
91. Black CA, Bucher ML, Bradner JM, Jonas L, Igarza K, Miller GW. Assessing Vesicular Monoamine Transport and Toxicity Using Fluorescent False Neurotransmitters. Chem Res Toxicol. 2021;34(5):1256-64.
92. Daina A, Michielin O, Zoete V. SwissADME: a free web tool to evaluate pharmacokinetics, drug-likeness and medicinal chemistry friendliness of small molecules. Scientific Reports. 2017;7(1):42717.
93. Daina A, Zoete V. A BOILED-Egg To Predict Gastrointestinal Absorption and Brain Penetration of Small Molecules. ChemMedChem. 2016;11(11):1117-21.

94. PRESTWICK CHEMICAL LIBRARY®: 1520 DRUGS MAINLY FDA-APPROVED Prestwick chemical [cited 2022 05.05]. Available from: https://www.prestwickchemical.com/screening-libraries/prestwick-chemical-library/.
95. Chi O, Wang G, Chang Q, Weiss H. Effects of isoproterenol on blood-brain barrier permeability in rats. Neurological Research. 1998;20(3):259-64.
96. Olesen J, Hougård K, Hertz M. Isoproterenol and propranolol: ability to cross the blood-brain barrier and effects on cerebral circulation in man. Stroke. 1978;9(4):344-9.
97. Li Y, Liu L, Li J, Xie L, Wang GJ, Liu XD. Transport of gatifloxacin involves Na+/Ca2+ exchange and excludes P-glycoprotein and multidrug resistance associated-proteins in primary cultured rat brain endothelial cells. European Journal of Pharmacology. 2009;616(1-3):68-72.
98. Marcianes P, Negro S, Garcia-Garcia L, Montejo C, Barcia E, Fernandez-Carballido A. Surface-modified gatifloxacin nanoparticles with potential for treating central nervous system tuberculosis. International Journal of Nanomedicine. 2017;Volume 12:1959-68.
99. Wykretowicz A, Guzik P, Wysocki H. Doxazosin in the current treatment of hypertension. Expert Opinion on Pharmacotherapy. 2008;9(4):625-33.
100. O'Neil ML, Beckwith LE, Kincaid CL, Rasmussen DD. The α1-Adrenergic Receptor Antagonist, Doxazosin, Reduces Alcohol Drinking in Alcohol-Preferring (P) Rats. Alcoholism: Clinical and Experimental Research. 2013;37(2):202-12.
101. Castañeda MS, Tonini R, Richards CD, Stocker M, Pedarzani P. Benzamil inhibits neuronal and heterologously expressed small conductance Ca2+-activated K+ channels. Neuropharmacology. 2019;158:107738.
102. Grønberg M, Terland O, Husebye ES, Flatmark T. The effect of prenylamine and organic nitrates on the bioenergetics of bovine catecholamine storage vesicles. Biochemical Pharmacology. 1990;40(2):351-5.
103. Roy B, Han J, Hope KA, Peters TL, Palmer G, Reiter LT. An Unbiased Drug Screen for Seizure Suppressors in Duplication 15q Syndrome Reveals 5-HT1A and Dopamine Pathway Activation as Potential Therapies. Biological Psychiatry. 2020;88(9):698-709.
104. Kountouras J, Sofianou D, Gavalas E, Sianou E, Zavos C, Meletis G, et al. Trimebutine as a potential antimicrobial agent: a preliminary in vitro approach. Hippokratia. 2012;16(4):347-9.
105. Robert X, Gouet P. Deciphering key features in protein structures with the new ENDscript server. Nucleic Acids Research. 2014;42(W1):W320-W4.

9 Appendix

9.1 Alignment of human VMAT1 and VMAT2

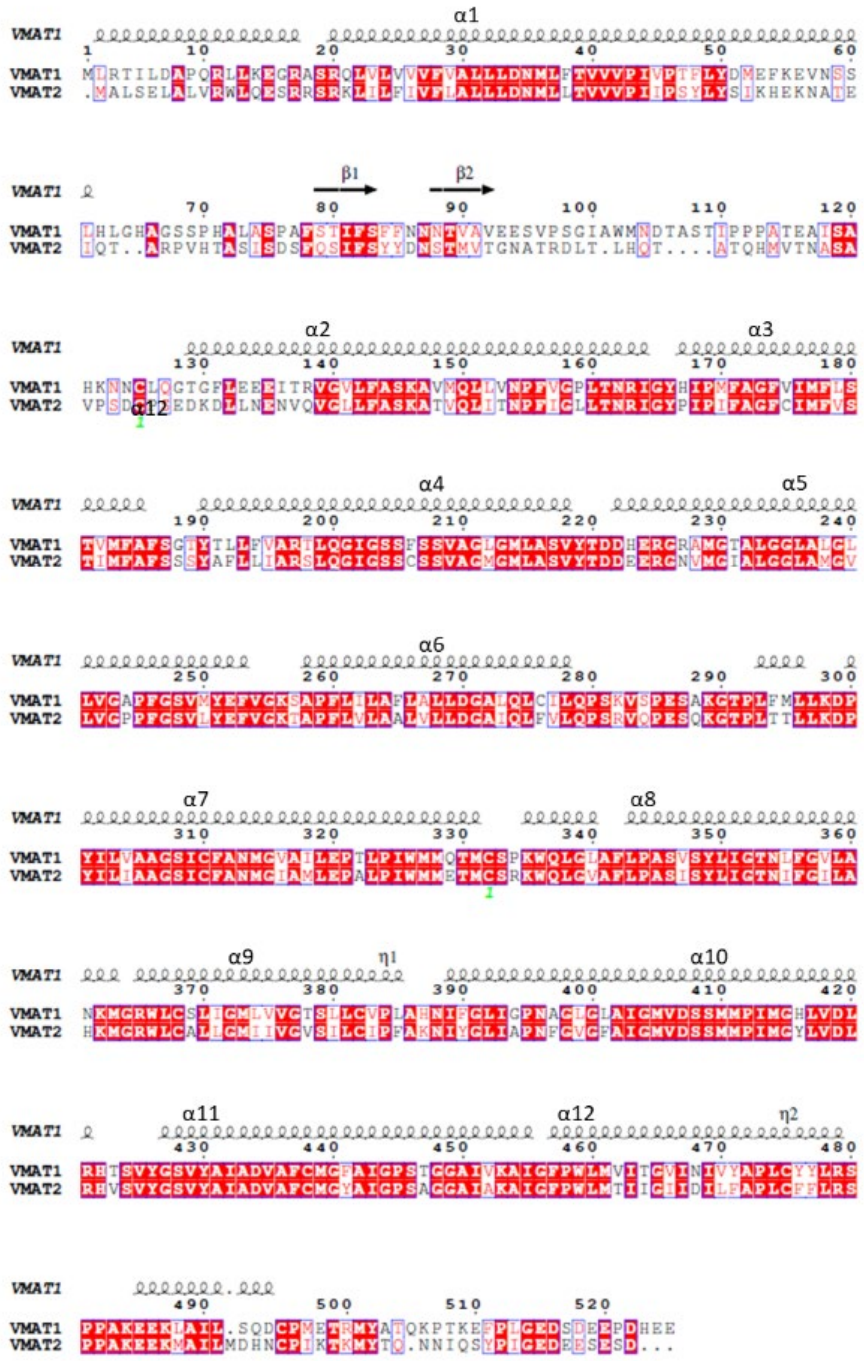

*Figure 9.1:**Alignment of human VMAT1 and VMAT2.** Aligned with Clustal Omega (8), with sequence from UniProt (P54219 and Q05940). Figure made with ESPript (105).*

9.2 Validation of hits from Prestwick chemical library®

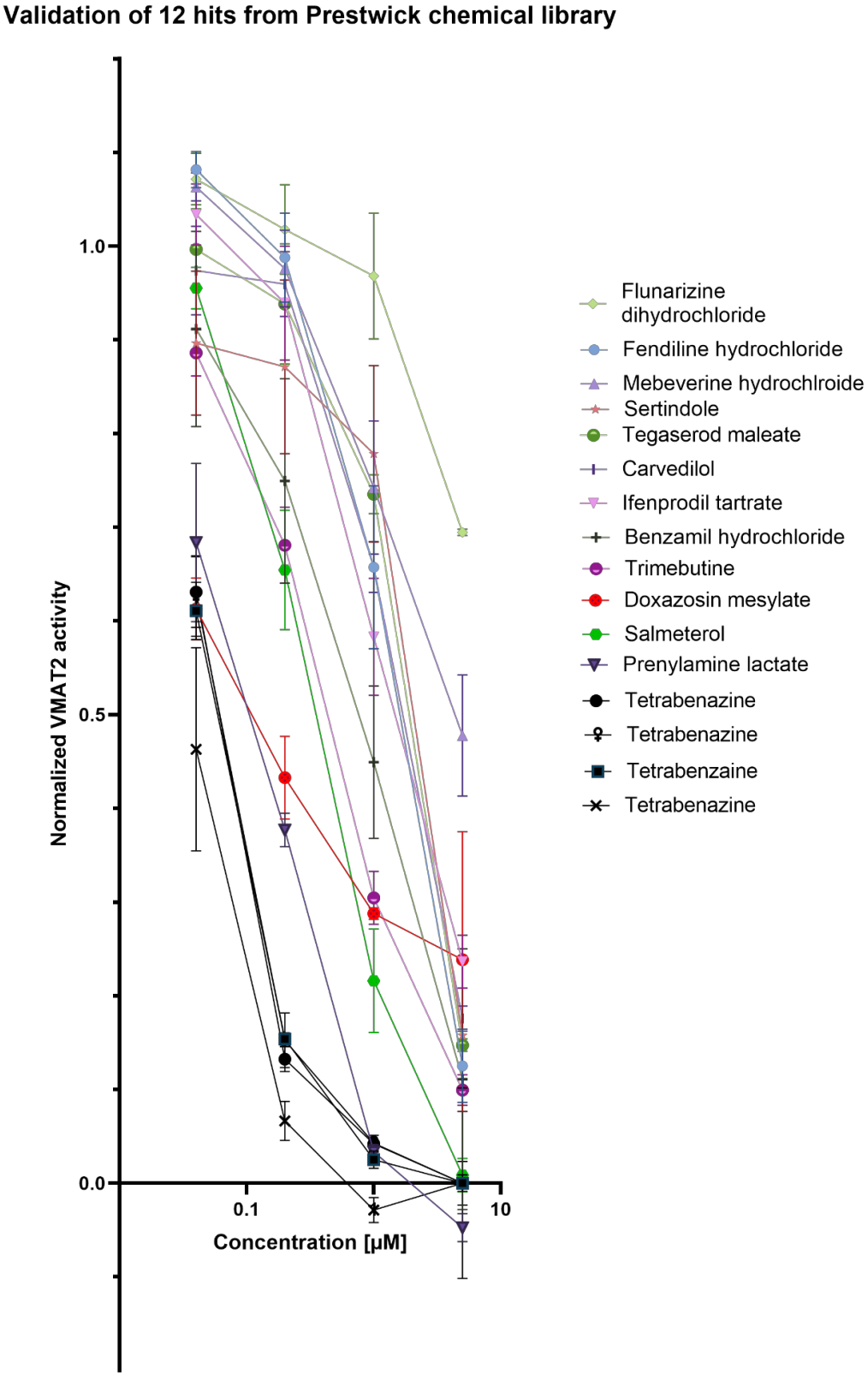

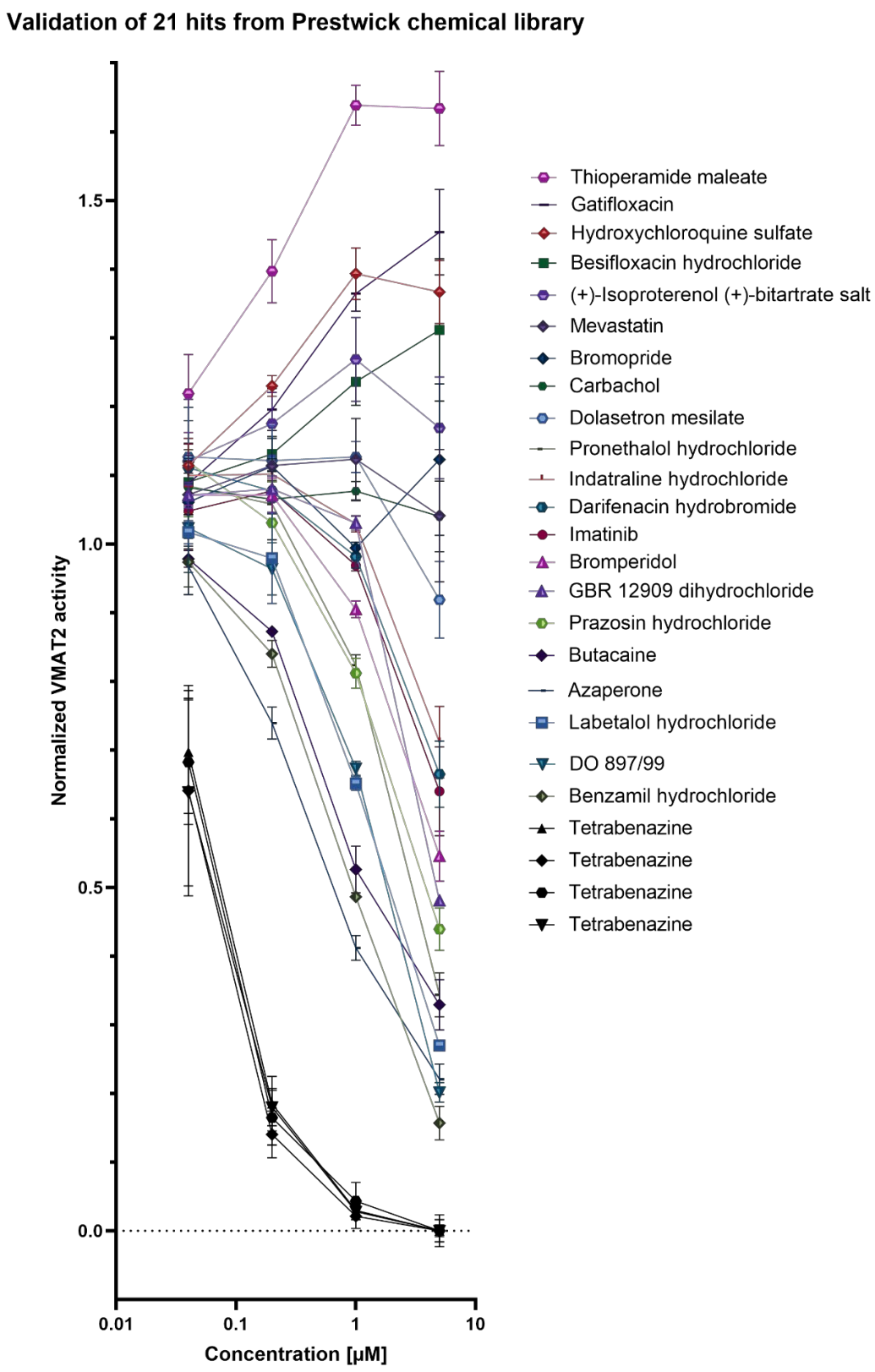

Figure 9.2: ***Concentration dependent validation of 33 of the initial hits.*** *Hits fulfilling the hit threshold of having activity higher or lower than 3 x STD and 5 x STD for the negative control from the initial screening, at both 1 and 5 µM were tested. The validation assay was also supplemented with other hits not fulfilling all the listed criteria.*

9.3 IC50 and EC50 Graphs

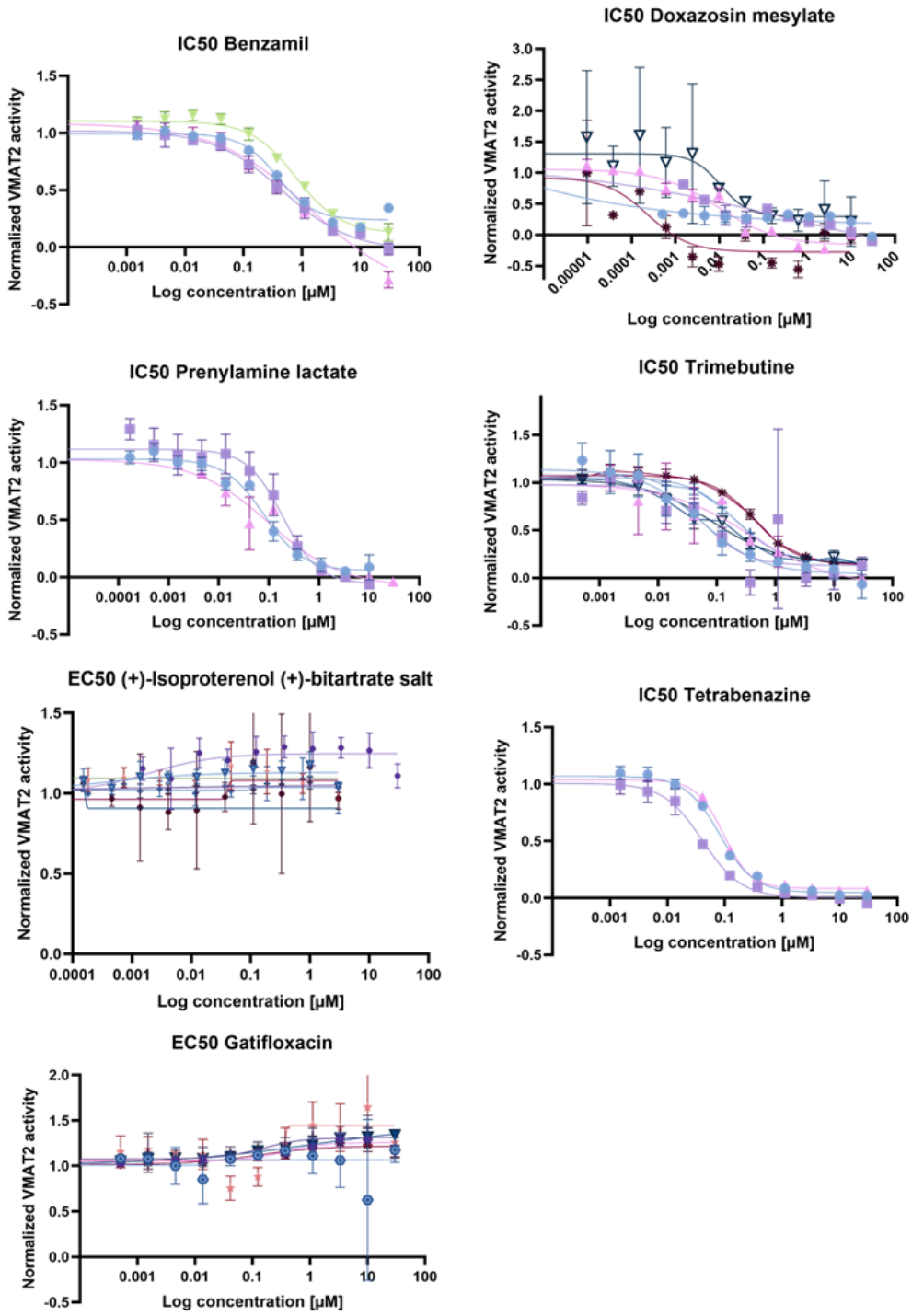

*Figure 9.3: **All IC_{50} and EC_{50} curves for VMAT2.** For benzamil, doxazosin mesylate, prenylamine lacate, trimebutine, (+)-isoproterenol (+)-bitartrate salt, gatifloxacin and tetrabenazine.*

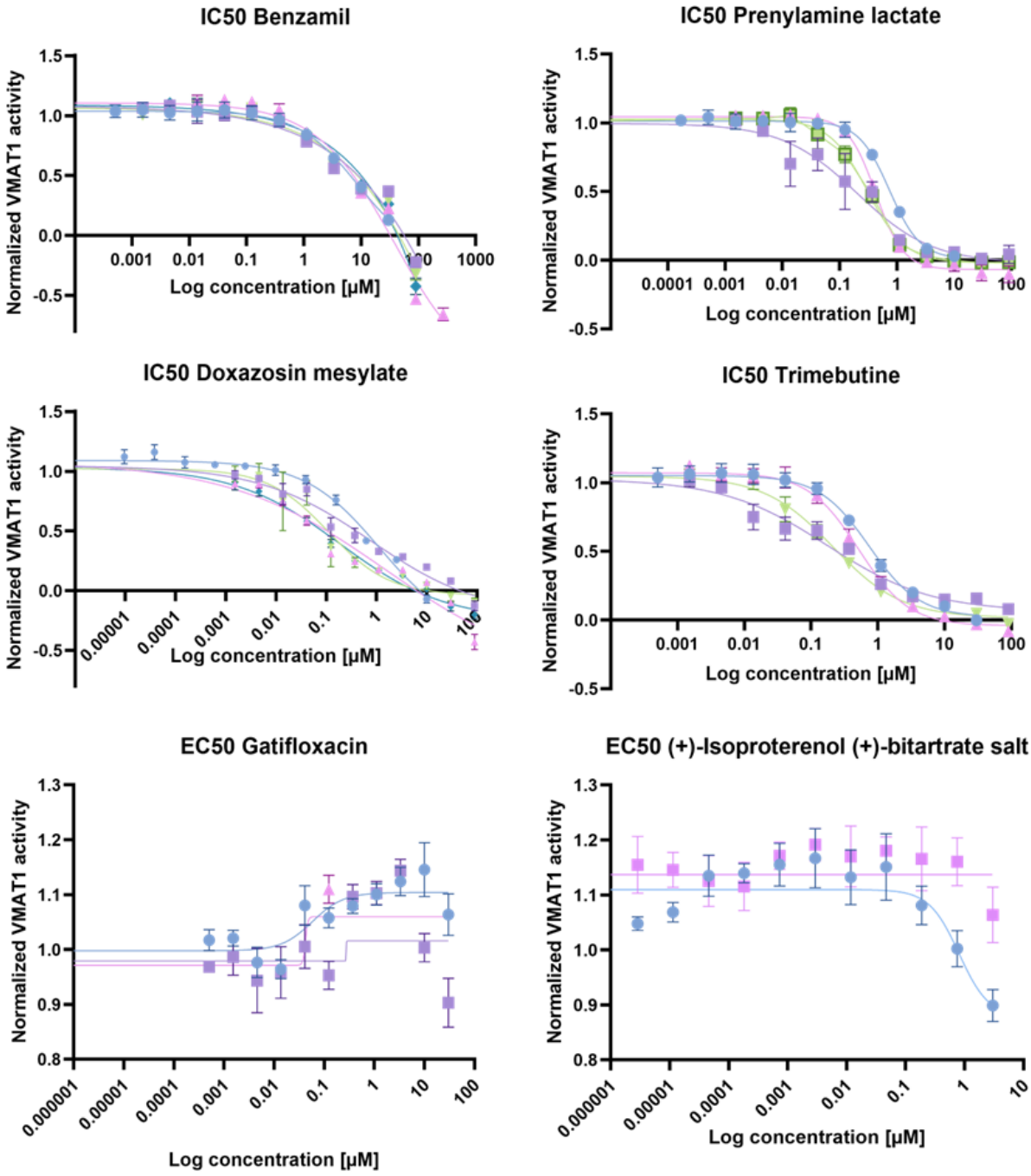

Figure 9.4: ***All IC_{50} and EC_{50} graphs for VMAT1.*** *The graphs represented demonstrates the difficulty of determine IC50 and EC50 for certain compounds.*